COSMOLOGY AND DEEP SURVEYS

ISO AND THE COSMIC INFRARED BACKGROUND

Hervé Dole

[1] SIRTF/MIPS Team, Steward Observatory, University of Arizona, 933 N Cherry Ave, Tucson, AZ, 85721, USA

ABSTRACT

ISO observed, for the first time to such a high sensitivity level, the mid- and far-infrared universe. A number of deep surveys were performed to probe the cosmological evolution of galaxies. In this review, I discuss and summarize results of mid-infrared ISOCAM and far-infrared ISOPHOT surveys, and show how our vision of the extragalactic infrared universe has become more accurate. In particular, ISO allowed us to resolve into sources a significant fraction of the Cosmic Infrared Background (CIB) in the mid-infrared, and to probe a fainter population in the far-infrared with the detection of the CIB fluctuations. Together with other wavelength data sets, the nature of ISO galaxies is now in the process of being understood.

I also show that the high quality of the ISO data put strong constraints on the scenarios of galaxy evolution. This induced a burst in the development of models, yielding to a more coherent picture of galaxy evolution.

I finally emphasize the potential of the ISO Data Archive in the field of observational cosmology, and describe the next steps, in particular the forthcoming cosmological surveys to be carried out by SIRTF.

Key words: ISO – infrared galaxies – galaxy evolution – extragalactic surveys – cosmic infrared background
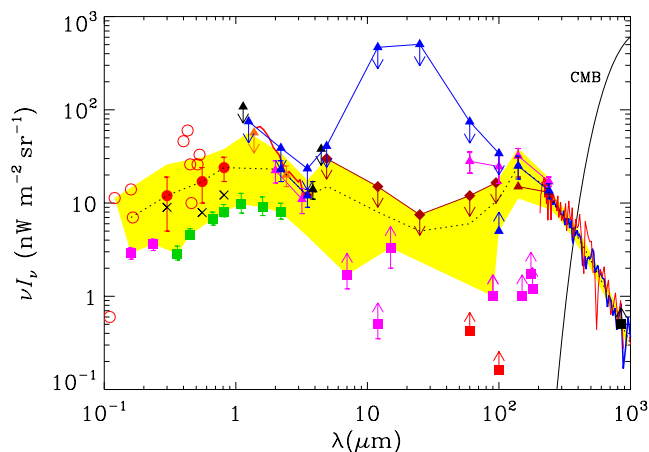
Figure 1. The Cosmic Infrared Background Spectral Energy Distribution from Hauser & Dwek (2001). This plot includes detection (solid line in the submm part), upper limits (triangles and diamonds), and lower limits from source counts (squares). The shaded region represents current observational limits, and the solid rising curve in the mm range represents the CMB.

1. INTRODUCTION

The Cosmic Infrared Background (CIB) (e.g. Puget et al. 1996; Hauser & Dwek 2001) is the relic emission of galaxy formation and evolution, being composed of light radiated from galaxies since their formation. The aim of the cosmological surveys is to resolve the CIB into sources, and to provide data on galaxies at various wavelengths, redshifts, with enough quality on individual objects as well as with statistical significant samples, in order to address the questions of the processes of galaxy formation and evolution, and the nature of the galaxies.

The CIB Spectral Energy Distribution (SED), shown in Fig. 1 (from Hauser & Dwek, 2001) shows the existence of a minimum between 3 and 10 μm separating direct stellar radiation from the FIR part due to radiation re-emitted by dust. The latter radiation contains at least a comparable integrated power as the former, and perhaps as much as 2.5 times more. This ratio is much larger than what is measured locally ($\sim$30%). The

CIB is thus likely to be dominated by a population of strongly evolving redshifted IR galaxies.

ISO revolutionized our view of the extragalactic universe with sensitive cosmological surveys carried out in the mid- and far- infrared. Of course, other cosmological surveys have been carried out with SCUBA, MAMBO, Chandra, XMM, and in the optical range; all give invaluable informations about galaxy evolution, but it is beyond the scope of this short paper to review them. Reviews of extragalactic results from ISO can be found in Genzel & Cesarsky 2000 and Franceschini et al. 2001, and a comprehensive overview of ISO operations and science in Casoli et al. (2000) (particularly in the Puget & Guiderdoni paper). I will here summarize the main results obtained in the MIR with ISOCAM (Sect. 2), in the FIR with ISOPHOT (Sect. 3), and overview the models that ISO data were able to constrain (Sect. 4). Sect. 5 emphasizes the potential of the ISO archive, and in Sect. 6 I briefly explore the future of IR (and mm) astronomy, in particular with SIRTF.
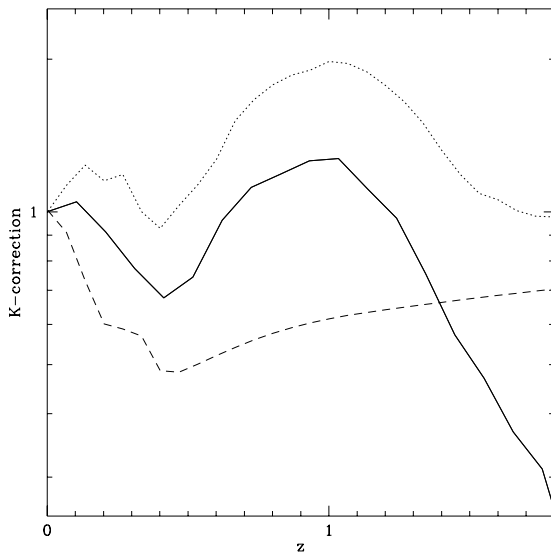
Figure 2. K-corrections from Francecshini et al. 2001. Dash: M82 spectrum at 7 μm. Dot: inactive spiral at 15 μm. Line: M82-like spectrum at 15 μm.

Figure 3. Differential source counts (normalized to Euclidean) at 15 μm from Elbaz et al. 1999. The shadowed area represents a scenario with no evolution. Symbols represent different surveys.

2. MID INFRARED SURVEYS

2.1. SPECIFICITIES

The mid-infrared surveys have been conducted with ISOCAM (Cesarsky et al. 1996), mainly at 7 and 15 μm; a few have been performed at 4.5 μm and 12 μm (Clements et al. 1999). At 7 μm using the LW2 filter (e.g. Taniguchi et al. 1997; Oliver et al. 2002), the contamination by stars is important and data at other wavelengths (usually near infrared) are needed to identify them. The decreasing k-correction is less favorable for detecting higher redshift galaxies (dash line in Fig. 2, taken from Franceschini et al. 2001).

At 15 μm using the LW3 filter (e.g Elbaz et al. 1999), the stellar contamination is less of a problem and the k-correction of galaxies is favorable for detecting sources up to redshifts around 1.4 (Fig. 2). Thus, a significant part of the extragalactic results are based on 15 μm observations.

2.2. SOURCE COUNTS

Source counts at 15 μm show an impressive consistency over four decades of flux between surveys of different depths (e.g. Elbaz et al. 1999, Gruppioni et al, 2002). Data come from large and shallow surveys like ELAIS (e.g. Serjeant et al, 2000), to narrower and deeper surveys (e.g. Serjeant et al, 1997, Aussel et al, 1999; Altieri et al, 1999). The number counts (summarized in Fig. 3 by Elbaz et al. 1999) are in excess by a factor of 10, at the 0.5 mJy level, compared to non evolution scenarios. The slope is steep ($\alpha = 3.0 \pm 0.1$ in the differential counts, for $S_\nu > 0.4$ mJy), and a turnover appears at $S_\nu = 0.4$ mJy. At fainter levels, the convergence (decrease) is fast.
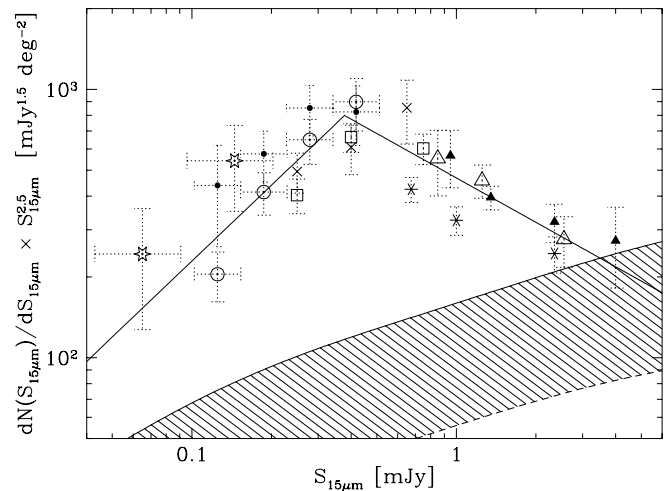

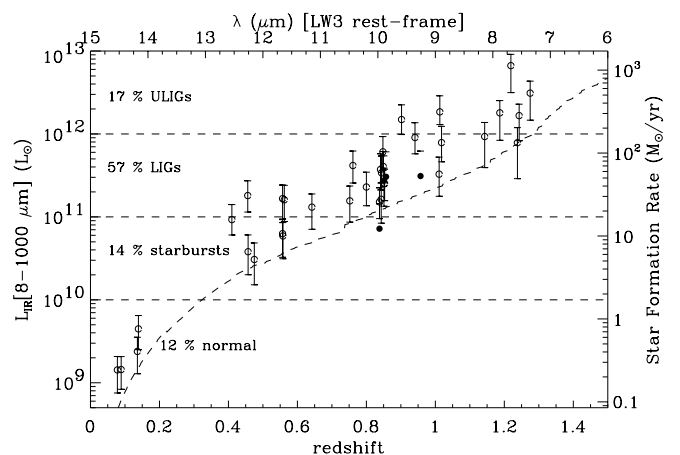*Figure 4. Infrared luminosity (left axis) and star formation rate (right axis, for starbursts only) of 15 μm $S > 0.1$ mJy galaxies in the HDF-N from Elbaz et al. 2002. The dash curve represents the sensitivity limit. This figure also illustrates the redshift distribution of the sources, with a median redshift of $z = 0.8$ (Aussel et al. 1999).*

2.3. NATURE OF THE GALAXIES

With a median redshift of $z \sim 0.8$ and most of the sources with $0.5 < z < 2$ (Aussel et al. 1999), the MIR sources have a mean luminosity of $6 \times 10^{11} L_\odot$ (Elbaz et al. 2002). Most of them are experiencing intense stellar formation of about 100 $M_\odot \mathrm{yr}^{-1}$, which appears to be uncorrelated with the faint blue galaxy population dominating the optical counts at z~0.7 (Ellis 1997; Elbaz et al. 1999). Fig. 4 (from Elbaz et al. 2002) represents their HDF-N sample, and summarizes the properties of MIR galaxies: redshift distribution, luminosity, and SFR (for 80% of the non-AGN galaxies).

2.4. GALAXY EVOLUTION

Elbaz et al. 2002 present a summary of the galaxy evolution at 15 μm and beyond. First, they show that 60% of the CIB at 15 μm is created by LIRGs ($L > 10^{11} L_\odot$). Second, they show that the comoving luminosity density at 15 μm was about 55 times larger at $z \sim 1$ than today. Third, still using some assumption about the SED of the galaxies, they conclude that the comoving density of IR luminosity radiated by dusty starbursts (which is directly related to the star formation) was about 70 ± 35 times larger at $z \sim 1$ than today. At intermediate redshifts, Flores et al. 1999 also determined the star formation rate. Finally, they show that about half of the CIB at 140 μm is produced by LIRGs and about one third by ULIRGs. Thus MIR galaxies observed by ISOCAM have resolved about 75% of the CIB at 140 μm.

3. FAR INFRARED SURVEYS

3.1. SPECIFICITIES

The far-infrared surveys have been conducted with ISOPHOT (Lemke et al., 1996), mainly at 90 and 170 μm; a few have been performed at 60, 120, 150 and 180 μm (Juvela et al. 2000; Linden-Voernle et al. 2000). In the 50 to 100 μm range, the C100 Ge:Ga camera is sensitive to the peak of rest-frame emission from obscured star formation. The decreasing k-correction, in addition to a challenging data processing, led to probe mainly the local universe. With 46 arcseconds per pixel and a FWHM of about the same size, the angular resolution at 100 μm is significant improved since IRAS.

In the 100 to 200 μm range, the C200 stressed Ge:Ga camera is sensitive to the very cool local galaxies as well as higher redshift starburst galaxies, thanks to an advantageous k-correction (e.g. Guiderdoni et al. 1997) and the behavior of the camera (e.g. Lagache & Dole, 2001). With 92 arcseconds per pixel and a FWHM of about the same size, the angular resolution at 170 μm is an issue for source identifications.

3.2. SOURCE COUNTS

Source counts at 170 μm (e.g. Kawara et al. 1998; Puget et al. 1999; Dole et al. 2001) exhibit a steep slope of $\alpha = 3.3 \pm 0.6$ between 180 and 500 mJy (lower left panel on Fig. 7) and, like in the MIR range, show sources in excess by a factor of 10 compared with no evolution scenario. This strong evolution was unexpected and quite difficult to reproduce with models. Matsuhara et al. 2000 extended the source count analysis to fainter fluxes and still detected a strong evolution.

At 60 and 90 μm, the situation is less clear, but preliminary source counts (Kawara et al. 1998; Efstathiou et al. 2000; Linden-Voernle et al., 2000) are compatible with no evolution scenarios on their bright end, and begin to show evolutionary effects on their bright end. New processing techniques (see Sect. 5) will certainly allow to go deeper.
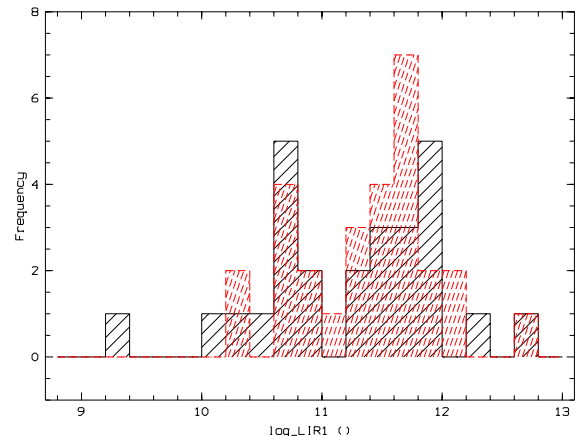

Figure 5. Distribution of IR luminosities from Patris et al (2002). Solid line: FIRBACK FSM 170 μm sample ($S > 200$ mJy); Dash: IRAS 100 μm sample from Bertin et al. 1997 with $110 < f_{60} < 200$ mJy.

3.3. NATURE OF THE GALAXIES

Determining the nature of the FIR galaxies has been a longer process than in the MIR, mainly because of the difficulty to find the shorter wavelength counterparts in a large beam. Various techniques have been used to overcome this problem, one of the most successful being the identification using 20cm radio data (e.g. Ciliegi et al. 1999). Another technique is the FIR multi-wavelength approach (Juvela et al., 2000) that helps constraining the position and the SED; it also helps to separate the cirrus structures from the extragalactic sources. A variation is to use ISOCAM and ISOPHOT data, like the ELAIS Survey (Oliver et al. 2000; Serjeant et al. 2000,2001). Finally, the Serendipity Survey (Stickel et al. 1998, 2000), by covering large and shallow areas, allows to detect many bright objects easier to follow-up or already known.

FIR ISO galaxies can be sorted schematically into two populations. First, the low redshift sources, typically $z < 0.3$ (e.g Serjeant et al., 2001; Patris et al. 2002, Kakazu et al. 2002), have moderate IR luminosities, below $10^{11} L_\odot$, and are cold (Stickel et al. 2000). Second, sources at higher redshift, $z \sim 0.3$ (Patris et al., 2002, see Fig. 5) and beyond, $z \sim 0.9$ (Chapman et al. 2002) are more luminous, typically $L > 10^{11} L_\odot$, and appear to be cold. Serjeant et al. (2001) derived the Luminosity Function at 90 μm, and started to detect an evolution compared to the local IRAS 100 μm sample.

3.4. FLUCTUATIONS OF THE CIB

Sources below the detection limit of a survey create fluctuations. If the detection limit does not allow to resolve the sources dominating the CIB intensity, which is the case in the FIR with ISO, characterizing these fluctuations gives very interesting information on the spatial correlations of these unresolved sources of cosmological significance. An example of the modeled redshift distribution of the unresolved sources at 170 μm
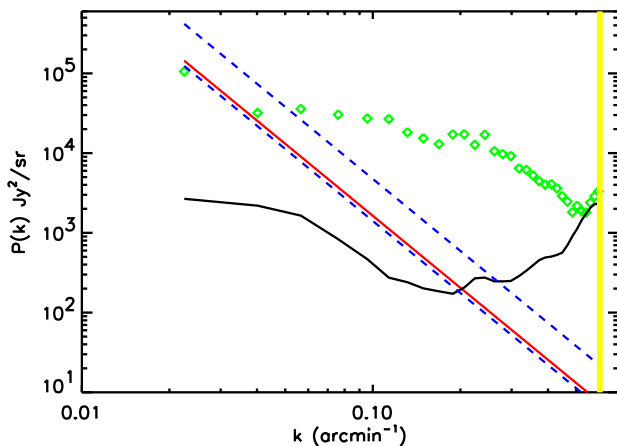
Figure 6. Fluctuations of the CIB in a power spectrum analysis of the FIRBACK/ELAIS N2 field at 170 microns by Puget & Lagache (2000). Observed power spectrum: diamond; straight continuous line: the best fit cirrus power spectrum; dash line: cirrus power spectrum deduced from Miville-Deschênes et al. 2002; continuous curve: detector noise.

can be found in Fig. 12 of Lagache et al. 2002; the sources dominating the CIB fluctuations have a redshift distribution peaking at $z \sim 0.9$. After the pioneering work of Herbstmeierer al (1998) with ISOPHOT, Lagache & Puget (2002) discovered them at 170 μm in the FIRBACK data, followed by other works at 170 and 90 μm (Matsuhara et al. 2000; Puget & Lagache, 2000; Kiss et al, 2001). Fig. 6 shows the CIB fluctuations in the FN2 field by Puget & Lagache, (2000), at wavenumbers $0.07 < k < 0.4$ arcmin^{-1}.

4. MODELS

ISO provided high quality data, taken in the frame of the cosmological survey programs, as well as nearby galaxies or serendipitous programs. The first observable to be widely used as a constraint on the models is the source counts at 15 and 170 μm, but also at 7 and 90 μm. The redshift distributions, mainly at 15 μm (and soon at 170 μm) put additional constraints, as well as a better knowledge of the nature of the galaxies: AGN vs Starburst, luminosities, star formation rate. The global star formation rate, as derived in part from ISOCAM data, adds other constraints to the models. Finally, a few models use explicitly the constraint of the level of the CIB fluctuations in the far infrared.

These observables and constraints induced a burst in the development of new models in the late nineties, among which: Roche & Eales (1999), Tan et al. (1999), Devriendt & Guiderdoni (2000), Dole et al. (2000), Wang (2000), Chary & Elbaz (2001), Franceschini et al. (2001), Malkan & Stecker (2001), Pearson (2001), Rowan-Robinson (2001), Takeuchi (2001), Xu et al. (2001), Balland et al. (2002), Lagache et al. (2002), Totani & Takeuchi (2002), Wang (2002). This development was also made possible because of the better knowledge of the galaxies

SED in the infrared (e.g. Dale et al. 2000; Helou et al. 2000; Lutz et al. 2000; Stickel et al. 2000, Tuffs & Popescu, 2002), with the availability of the SED of the CIB (Gispert et al. 2000; Hauser & Dwek, 2001), and of complementary data sets (X-rays, optical, NIR, submm, radio).

Even if there is no unique scenario reproducing all the observables, the models help now to have a more coherent picture of galaxy evolution. It is beyond the scope of this paper to review the models and their predictions, we thus give here only two examples. Fig. 7 shows the observed source counts at 15, 60, 170 and 850 μm and the fits by Lagache et al. 2002. Using other kind but similar evolutions (pure density and pure luminosity evolutions in addition to the density+luminosity evolution), Chary & Elbaz (2001) predict the star formation rate and compare it with data and Xu et al (2001) (Fig. 8). Combined with the different approach of Gispert et al (2000), the SFR is well constrained in the redshift range $1 < z < 3$.
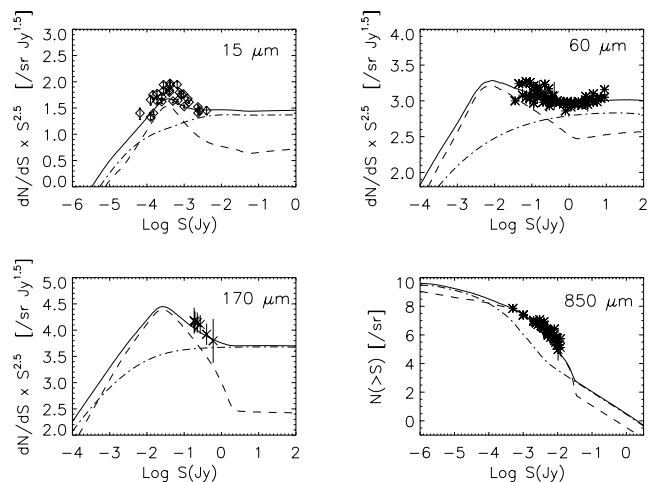

Figure 7. Observed source counts at 15, 60, 170 and 850 μm with the model of Lagache et al. 2002. Symbols represent data (CAM at 15 μm, IRAS at 60 μm, PHOT at 170 μm and SCUBA at 850 μm. Solid line: model prediction. Dash: LIRG/starburst component. Dot-dash: normal/cold galaxy component.

5. POTENTIAL OF ISO DATA

Even if the ISO data led to an impressive scientific return with a high efficiency (about 62% of the data are published) in the field of the cosmological evolution of the galaxies, many other results are still to come, based on the amount of unpublished data available in the archive.

In addition, new techniques of data reduction are now available, thanks to a better understanding of detector behaviors, both for the Silicon Array (CAM)(Coulais & Abergel, 2000; Miville-Deschênes et al. 2000; Lari et al. 2001, 2002; Vaccari, 2002) and the Germanium detectors (PHOT) (Coulais et al. 2000). Processing unpublished data and/or reprocessing published data allows us to reach better sensitivity levels with a

Figure 9. Predicted redshift distribution of sources observed at 24 μm with MIPS on SIRTF, from Dole et al. 2002, for various 5σ surveys depths. Line: GTO shallow survey or SWIRE. Dash: GTO deep. Dot: GTO ultradeep or GOODS.
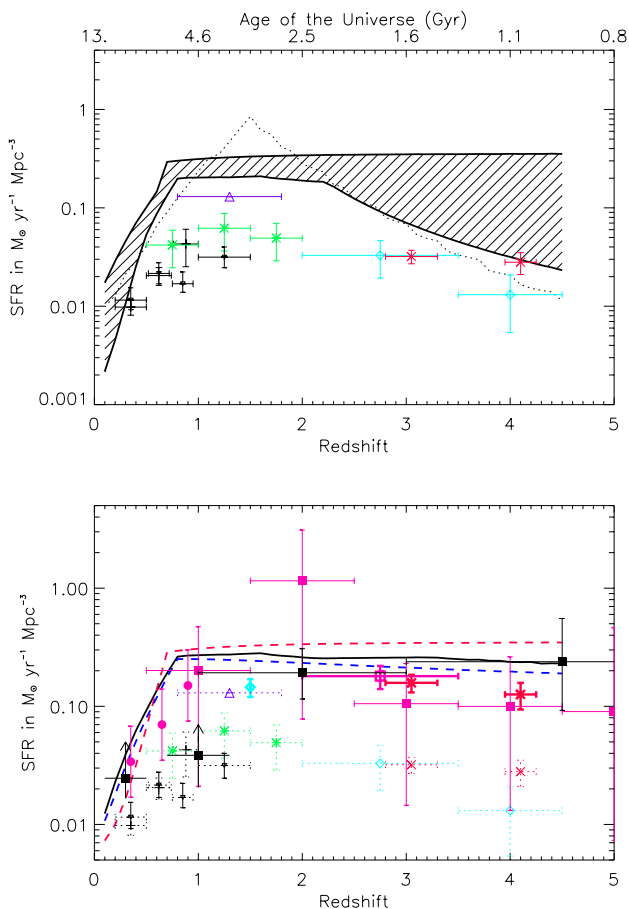

Figure 8. Star Formation Rate from Chary & Elbaz (2001). Upper panel: min and max range from their model, and observed UV/opt data; dots represent Xu et al. 2001 model. Lower panel: 3 different evolution scenarios from their model and data corrected for extinction. Line: pure luminosity; upper dash: pure density; lower dash: luminosity+density.

6. THE NEXT STEPS: SIRTF AND BEYOND

SIRTF, the Space Infrared Telescope Facility, to be launched in early 2003, is expected to improve our view of the IR universe over the next five years, thanks to the recent technological developments in IR detector arrays. A number of multiwavelength cosmological surveys are scheduled with MIPS (Multiband Imaging Photometer for SIRTF) at 24, 70 and 160 μm (Dole et al. 2002[1]) and IRAC (Infrared Array Camera) at 3.6, 4.5, 5.8 and 8.0 μm. In the frame of the Guaranteed Time (GTO) or Legacy (GOODS and SWIRE) Surveys, about 80 Sq. Deg. will be observed at different depths. Probing the properties of the galaxies with samples of statistical significance up to redshifts of 2.5 or more will be possible. Fig. 9 (from Dole et al, 2002) shows predictions of the redshift distribution at 24 μm for MIPS surveys.

The next steps after ISO and SIRTF for understanding the infrared and submillimeter Universe from space will be ISAS's ASTRO-F in 2004, ESA's Herschel & Planck (around 2007), and NASA's NGST (around 2010+), in addition to the ground-based ALMA (from 2005). These telescopes are the promise for a lot of exciting science to be done (at least) in the next 15 years !

higher confidence (e.g. for ISOCAM HDF-N: Serjeant et al. 1997; Aussel et al. 1999; Désert et al. 1999. E.g. for ISOPHOT Lockman Hole: Kawara at al., 1998; Rodighiero et al. 2002).

Concerning the CIB and the cirrus foreground, a brilliant example of what can be done from the archive is the work of Kiss et al (2001,2002), detailed in this conference. Furthermore, the ISO data may induce discoveries in other data sets. A recent example concerns the fluctuations of the CIB in the far infrared. Lagache & Puget (2000) and Puget & Lagache (2000) measured the level of the fluctuations of the CIB at 170μm in the FIRBACK fields. Given the SED of the CIB, it was possible to predict the fluctuation level at 60 and 100 μm (e.g. Lagache, Dole, Puget, 2002), and show that this might be detectable in the IRAS data. As a consequence, Miville-Deschênes et al. (2002) recently reported the first detection of the CIB fluctuations at 60 and 100 μm in the IRAS data.
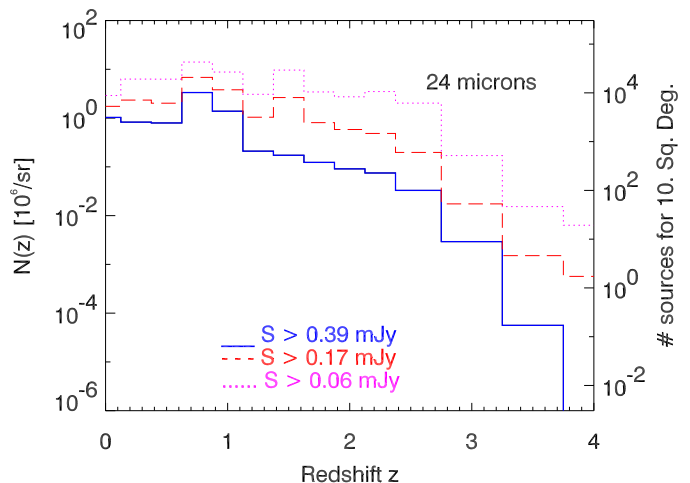
---

[1] see also http://lully.as.arizona.edu

312

REFERENCES

Altieri B., Metcalfe L., Kneib J-P. et al., 1999, A&A, 343, L65

Aussel H., Cesarsky C.J., Elbaz D., et al., 1999, A&A, 342, 313

Balland C., Devriendt, J., Silk J., 2002, MNRAS, Submitted, astro-ph/0210030

Bertin E., Dennefeld, M. & Moshir, M., 1997, A&A, 323, 685

Casoli F., Lequeux J., David F., Eds, 'Infrared Space Astronomy, Today and Tomorrow', Les Houches Summer School LXX, EDP Sciences, Springer-Verlag, 2000

Cesarsky C., Abergel, A., Agnese P., et al., 1996, A&A, 315, L32

Chapman, S. C., Smail I., Ivison R., et al., 2002, ApJ, 573, 66

Chary R., & Elbaz D., 2001, ApJ, 556, 562

Ciliegi P., McMahon R. G., Miley G., et al., 1999, MNRAS, 302, 222

Clements D., Desert F-X., Franceschini A., et al., 1999, A&A, 346, 383

Coulais A., & Abergel A., 2000, A&AS, 141, 533

Coulais A., Fouks B. I., Giovannelli J. F., et al., 2000, A&A, SPIE

Dale D., Silbermann, N., Helou, G., et al., 2000, AJ, 120, 583

Désert F-X., Puget J-L., Clements D., et al., 1999, A&A, 342, 363

Devriendt J.& Guiderdoni B., 2000, A&A, 363, 851

Dole H., Gispert R., Lagache, G., et al., 2000, Springer Lect. Notes in Ph., v548, 54, astro-ph/0002283

Dole H., Gispert R., Lagache, G., et al., 2001, A&A, 372, 364

Dole H., Lagache G., Puget J-L., 2003, ApJ, in press, astro-ph/0211312

Efstatiou A., Oliver S., Rowan-Robinson M., et al., 2000, MNRAS, 319, 1169

Elbaz D., Cesarsky C., Fadda D., et al., 1999, A&A, 351, L37

Elbaz D., Flores H., Chanial P., et al., 2002, A&A, 384, 848

Ellis R. S., 1997, ARAA, 35, 389

Flores H., Hammer F., Thuan T. X., et al., 1999, ApJ, 517, 148

Franceschini A., Aussel H., Cesarsky C., et al., 2001, A&A, 378, 1

Genzel R., & Cesarsky C., 2000, ARAA, 38, 761

Gispert R., Lagache G., Puget J-L., 2000, A&A, 360, 1

Gruppioni C., et al, 2002, MNRAS, 335, 831

Guiderdoni B., Bouchet F. R., Puget J-L., et al., 1997, Nature, 390, 257

Hauser M.,& Dwek E., 2001, ARAA, 37, 249

Helou G., Lu N. Y., Werner M. W., et al., 2000, ApJ, 532, L21

Herbstmeierer U., Abraham P., Lemke D., et al., 1998, A&A, 332, 739

Juvela M., Mattila K., Lemke D., 2000, A&A, 360, 813

Kakazu Y., Sanders D., Jpseph R., et al., 2002, A&A, IAU184, astro-ph/0201326

Kawara K., Sato Y., Matsuhara H., et al., 1998, A&A, 336, L9

Kiss C., Abraham P., Klaas, U., et al., 2001, A&A, 379, 1161

Kiss C., et al., 2002, this conference

Lagache G. & Puget J-L., 2000 , A&A, 355, 17

Lagache G. & Dole H., 2001, A&A, 372, 702

Lagache G., Dole H., Puget J-L., 2002, A&A, MNRAS, in press, astro-ph/0209115

Lari C., Pozzi F., Gruppioni C., et al., 2001, A&A, 325, 1173

Lari C., et al., 2002, this conference

Lemke D., Klaas U., Abolins J., et al., 1996, A&A, 315, L64

Linden-Voernle M. J. D., Norgaard-Nielsen H. U., Jorgensenet H. E., al., 2000, A&A, 359, L51

Lutz D., 2000, New As. Rev., 44, L241

Malkan M., & Stecker F., 2001, ApJ, 555, 641

Matsuhara H., Kawara K., Sato Y., et al., 2000, A&A, 361, 407

Miville-Deschênes M-A., Boulanger F., Abergel A., et al., 2000, 146, 519

Miville-Deschênes M-A., Lagache G., Puget J-L., 2002, 393, 749

Oliver S., Rowan-Robinson, M., Alexander D., et al., 2000, MNRAS, 316, 749

Oliver S., Mann R. G., Carballo R., et al., 2002, MNRAS, 332, 536

Patris J., Dennefeld M., Lagache G., et al., 2002, A&A, submitted

Pearson C., 2001, MNRAS, 325, 1511

Puget J-L., Abergel A., Bernard J-P., et al., 1996, A&A, 308, L5

Puget J-L., Lagache G., Clements D., et al., 1999, A&A, 345, 29

Puget J-L.,& Lagache G., 2000, A&A, IAU204, astro-ph/0101105

Roche N., & Eales S., 1999, MNRAS, 307, 111

Rodighiero G., et al., 2002, this conference

Rowan-Robinson M., 2001a, New As. Rev., 45, 631

Rowan-Robinson M., 2001b, ApJ, 549, 745

Serjeant S., Eaton N., Oliver S., et al., 1997, MNRAS, 289, 457

Serjeant S., Oliver S., Rowan-Robinson M., et al., 2000, MNRAS, 316, 768

Serjeant S., Efstathiou A., Oliver S., et al., 2001, MNRAS, 322, 262

Stickel M., Bogun S., Lemke D., et al., 1998, A&A, 336, 116

Stickel M., Lemke D., Klaas U., et al., 2000, A&A, 359, 865

Takeuchi T., Ishii T., Hirashita H., et al., 2001, PASJ, 53, 37

Tan J., Silk J., Balland C., 1999, ApJ, 522, 579

Taniguchi Y., Cowie L., Sato Y., et al., 1997, A&A, 328, L9

Totani T., & Takeuchi T., 2002, ApJ, 570, 470

Tuffs R., & Popescu C., 2002, this conference

Vaccari M., et al., 2002, this conference

Xu C., Lonsdale C., Shupe D., et al., 2001, ApJ, 562, 179

Wang Y., Biermann P., 2000, A&A, 356, 808

Wang Y., 2002, A&A, 383, 755

A MID-INFRARED LOOK THROUGH THE LOCKMAN HOLE

Dario Fadda[1,2]**, Carlo Lari**[3]**, Giulia Rodighiero**[4]**, David Elbaz**[5]**, Hector Flores**[6]**, Alberto Franceschini**[4]**,
Catherine Cesarsky**[7]**, and Ismael Perez-Fournon**[2]

[1] Caltech, SIRTF Science Center, MC 220-6, Pasadena, CA 91126, USA
[2] Instituto de Astrofísica de Canarias (IAC), Via Lactea S/N, E-38200 La Laguna, Spain
[3] Istituto di Radioastronomia del CNR (IRA), via Gobetti 101, I-40129 Bologna, Italy
[4] Dipartimento di Astronomia, Università di Padova, Vicolo dell'Osservatorio 5, I-35122 Padova, Italy
[5] CEA, DSM, DAPNIA, Service d'Astrophysique, F-91191 Gif-sur-Yvette Cedex, France
[6] DAEC/LUL, Observatoire de Paris-Meudon, 5 place Jules Janssen, F-92195 Meudon, France
[7] European Southern Observatory (ESO), Karl-Schwarzschild-Strasse, 2, 85748 Garching bei München, Germany

ABSTRACT

More than half square degree in the region of the Lockman Hole has been observed at 14.3μm with the ISOCAM camera on board ISO. We analyzed these data using the algorithm by Lari et al. (2001) detecting more than 270 sources with fluxes between 0.2 and 4 mJy. Thanks to ancillary optical data obtained with the wide field camera of the Isaac Newton telescope, we are able to find clear optical counterparts for 93% of the infrared sources. In the flux range where the survey is more than 80% complete (fluxes greater than 0.8 mJy), the counts are in good agreement with the recent results of Gruppioni et al. (2002) in the ELAIS South field.

Key words: ISO – surveys – extragalactic

1. INTRODUCTION

IRAS and COBE experiments showed that a large part of the bolometric luminosity from the deep Universe is absorbed by dust and reprocessed into the infrared wavelengths (Soifer & Neugebauer 1991, Puget et al. 1996). This process is especially important in galaxies or galaxy regions where stars are forming in great quantity. Therefore, an infrared image of the deep Universe can be seen as a complementary image of the usual optical images, revealing the sources that are heavily obscured in the optical wavelengths.

Unfortunately, only a few selected regions in the sky allow us to take a look at the deep Universe because of the presence of HI clouds in our own Galaxy, the so called "cirri" (*cirrus* means "curl" in Latin). One of these "holes" among clouds has been discovered by Lockman et al. (1986) and has been since then observed in several wavelengths from radio (with VLA, de Ruiter et al. 1997) to the X-rays (ROSAT observations, Hasinger et al. 1993 and more recently with XMM, Hasinger et al. 2001).

As part of the ISOCAM extragalactic guaranteed time surveys, a region of $44' \times 44'$ has been observed with the LW3 broad filter (centered at 14.3μm) with the ISOCAM camera (Cesarsky et al. 1996) on board ISO (Kessler et al. 1996). This has been the largest and shallowest of the surveys performed in this program.

Accordingly to the estimates of Elbaz et al. (2002), the sources that are detected with this survey account for 20% of the total cosmic infrared background. Moreover, the flux range which is explored by this survey corresponds to the region where there is a change in the slope of the LW3 counts (see Elbaz et al. 1999) which can be explained only with a strong evolution in number and density of the galaxies.

The interest in studying the optical counterparts of the galaxies detected in this survey is therefore evident. Only a multi-wavelength approach can give us the necessary information to understand the nature of these strong infrared emitters.

The same area has been also covered by other ISO observations: 90μm and 160μm observations (Kawara 1998, see also the contribution of Rodighiero in the same volume) and deep LW3 (14.3μm) and LW2 (6.7μm) observations in a smaller region (Fadda et al., in preparation). If we take into account also the observations made in the sub-mm wavelength by SCUBA (Scott et al. 2002), the Lockman Hole region is one of the few regions in the sky which have been deeply observed at every accessible wavelength.

2. OBSERVATIONS

The survey consists of 4 raster scans totaling 55 ksec with the mid-infrared camera ISOCAM in the direction
RA(J2000)=10:52:03 DEC(J2000)=+57:21:46 .
Each of the four scans consists of 24×8 sub-pointings, with 11 readouts of 5 seconds of exposure time. The pixel size of these observations is 6 arcseconds in order to optimize the angular resolution of the camera and the signal-to-noise ratio for the detection of faint sources.

In order to study the ISOCAM sources, a deep Sloan r image has been obtained with the wide field camera (WFC) of the Isaac Newton Telescope at La Palma, Spain. The image was obtained with four pointings of the camera repeated 5 times to fill the gaps, correct for bad pixels and cosmic rays for a total of 4 hours of integration.

3. DATA ANALYSIS

The ISOCAM data have been reduced using the recent technique developed by Lari et al. (2001, see also the contribution of Vaccari in the same volume). This technique is especially suited for the detection of faint sources in observations with
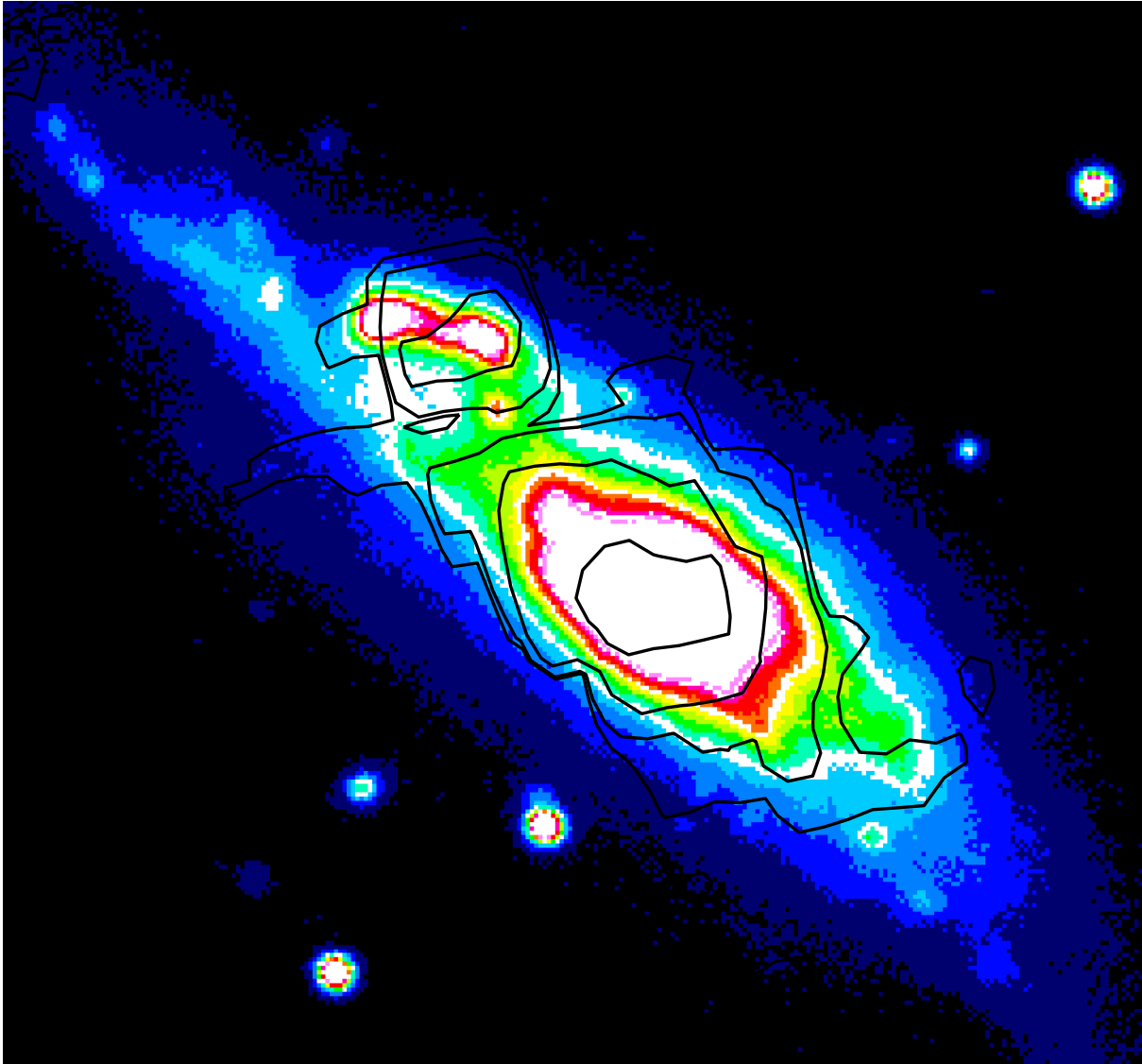
Figure 1. NGC 3440, the only IRAS source in the field observed by ISOCAM. The infrared emission (black isocontours) is resolved in two spots, while the shallowest contours show the structure of the arms. A careful inspection allows one to note that the optical arms are counter-rotating with respect to the infrared arms.

low redundancy, which is the case of the Lockman Hole Shallow survey. Our final catalog contains 277 sources at the 5σ level in the signal-to-noise map, with fluxes between 0.2 and 4 mJy. To appreciate the level of refinement of the analysis, Fig. 1 shows the isocontours of the unique IRAS source in the field. The source appears resolved in two components. The arms are also visible and seem to be counter-rotating with respect to the optical ones.

The reduction method computes the photometry correcting the peak flux measured on the map through a simulation of a source of the same flux and in the same position where it has been detected (called auto-simulation). The ratio between input and measured fluxes of the auto-simulated source allows one to correct the flux of the real source taking into account the local problems around the source. However, since the measured

positions always differ from the real ones, fluxes are on average underestimated. It is possible to quantify this bias by simulating false sources in the raw data.

According to our simulations, fluxes are underestimated by 12%. After the correction for this bias, fluxes of stars in the field agree fairly well with the LW3 fluxes computed on the basis of their optical and near-IR colors.

The analysis of the optical data has been done with the IRAF package MSCRED and using the information about the features of the camera in the web page of the Wide Field Survey (www.ast.cam.ac.uk/ wfcsur/index.php) . The source extraction has been made using Sextractor (Bertin & Arnouts 1996).
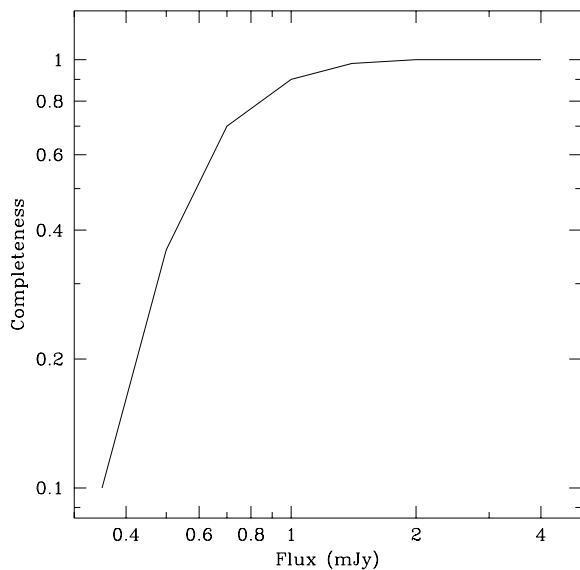
Figure 2. Completeness as a function of the flux from simulations done adding false sources to the raw data cube.

4. COUNTS

In absence of a complete identification of the optical counterparts and measurement of the redshifts, counts are the main tool to study the galaxy evolution providing constrains to the theoretical models. The LW3 counts based on a preliminary reduction of ISOCAM data by Elbaz et al. (1999) showed a clear departure from Euclidean prediction at fluxes less than 1 mJy. This has been interpreted as an evidence for a strongly evolving population of mid-IR galaxies (Franceschini et al. 2001).

Sources in the Lockman Shallow Survey span a flux range between 0.2 and 4 mJy. To study the completeness of the survey, extensive simulations have been performed adding false sources to the original cube of data at several fluxes (0.35, 0.5, 0.7, 1., 1.4, 2., 2.8 and 4 mJy). As shown in Fig. 2, the survey is 80% complete for fluxes greater than 0.8 mJy. Moreover, due to the limited area covered by the survey, counts make sense only for fluxes less than 2 mJy. In fact, if we exclude stars, there are only a few sources with fluxes greater than 2 mJy. Therefore, we estimate counts only between 0.8 and 2 mJy.

The star-galaxy separation in our catalog has been done on the basis of the shape of optical counterparts in the deep r-image: 12% of the sources are stars. The good quality of the image allowed us to identify more stars than those found in the counts by Elbaz et al. (1999). The counts we derived are in fact lower than those published by Elbaz et al. (1999). The main reason is the better star-galaxy separation although the fluxes also appear slightly overestimated in the previous analysis (around 10%).

If we compare our result with the recently published counts in the South ELAIS field (Gruppioni et al. 2002) we have a remarkable agreement. We stress the importance of our result since the ELAIS survey is far from completeness in the flux range covered by our survey (see Lari et al. 2001, Fig. 15). For instance, at 1 mJy the repeated central region of the ELAIS South survey which has a size comparable to the Lockman Hole Shallow survey is less than 60% complete. The other parts of the survey are only 20% complete (cfr. Lari et al. 2001, Fig. 9).
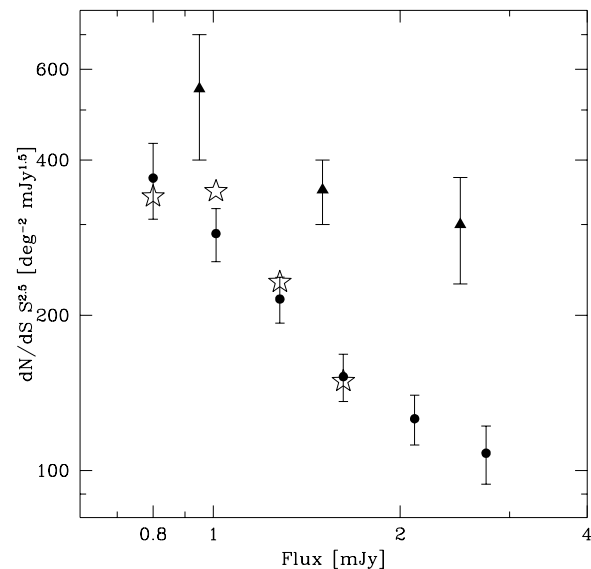

Figure 3. Differential LW3 extragalactic counts normalized to the Euclidean distribution ($N(S) \propto S^{-2.5}$). Counts from Elbaz et al. (1999) for the Lockman Shallow Survey (black triangles) and from Gruppioni et al. (2002) for the ELAIS South field (black dots) are compared with preliminary counts from our analysis (empty stars).

5. CONCLUSIONS

We have presented the analysis of the LW3 ($14.3\,\mu$m) ISOCAM Lockman Hole shallow survey done with the technique by Lari et al. (2001). We detect 270 sources with fluxes ranging between 0.2 and 4 mJy which have in 93% of the cases a clear optical counterpart in deep r images.

Through extensive simulations we estimated the completeness of the survey at different flux limits. In particular, the survey is 80% complete for fluxes greater than 0.8 mJy. The star contamination of this field is low (around 12%). After excluding stars on the basis of their shape and visual inspection on optical images, we derived the counts in the flux interval between 0.8 and 2 mJy. Our result agrees well with the counts by Gruppioni et al. (2002) in the ELAIS South field while they are lower than those published in Elbaz et al. (1999). The main difference with the analysis in Elbaz et al. (1999) is a better star/galaxy separation thanks to our recently obtained deep r images and an estimate of the flux slightly lower (around 10%) than the previous values (See Fig. 3).

316

REFERENCES

Bertin E. & Arnouts S., 1996, A&A Supp. 117, 393
Cesarsky C. J., Abergel A., Agnése P. et al., 1996, A&A 315, L32
de Ruiter H. R., Zamorani G., Parma P. et al., 1997, A&A 319, 7
Elbaz D., Cesarsky C. J., Fadda D. et al., 1999, A&A 351, L37
Elbaz D., Cesarsky C. J., Chanial P. et al., 2002, A&A 384, 848
Franceschini A., Aussel H., Cesarsky C. et al., 2001, A&A 378,1
Gruppioni C., Lari C., Pozzi F. et al., 2002, MNRAS 335, 831
Hasinger G., Burg R., Giacconi R. et al., 1993, A&A 275, 1
Hasinger G., Altieri B., Arnaud M. et al., 2001, A&A 365, 45
Kawara K., Sato Y., Matsuhara H., 1998, A&A 336, L9
Kessler M., Steinz J., Anderegg M. et al., 1996, A&A 315, L27
Lari C., Pozzi F., Gruppioni C. et al., 2001, MNRAS 325, 1173
Lockman, F. J., Jahoda, K., McCammon, D., 1986, ApJ, 302, 432
Puget J.-L., Abergel A., Bernard J.-P. et al., 1996, A&A 308, L5
Scott S. E., Fox M. J., Dunlop J. S. et al., 2002, MNRAS, 331, 817
Soifer B. T. & Neugebauer G., 1991, AJ, 101, 354

ISO LENSING STUDIES: BACKGROUND GALAXIES AND FOREGROUND CLUSTER PROPERTIES

Ricardo Perez-Martinez

XMM-Newton Science Operations Centre, European Space Agency, Villafranca del Castillo, P.O. Box 50727, 28080 Madrid, Spain.

for the ISO ARCS consortium

ABSTRACT

A number of ISO programmes, totaling over 100 hours of observation time, made use of the gravitational lensing phenomenon to extend the sensitivity of ISO observations. Substantial results derived from those programmes have been published, or are in the peer review process, addressing the MIR properties of the background lensed galaxy population. These results, which have important implications for galaxy evolution, and which resolve a large fraction of the 15 and $7\,\mu m$ infrared-background light, will be briefly summarised. But the data has much further potential. Little has been published to date concerning the implications of the ISO lensing data for the foreground clusters themselves, nor addressing the overlap between the observed ISO sources and lensed populations seen at X-Ray and Sub-mm wavelengths. We report briefly on an ongoing programme to systematically reassess the set of ISO observations of lensing galaxy clusters and to describe and compare the IR properties of the clusters themselves. The overlap between ISO source lists and recently published lists of X-Ray and Sub-mm sources in the same fields is under study.

Key words: Surveys – gravitational lensing – Galaxies: clusters: – Infrared: galaxies

1. INTRODUCTION

After the identification of the first cosmological gravitational lens by Young et al. (1980) there has been a rapid exploitation of both the theoretical and observational aspects of this phenomenon. Paczynśky attributed a lens origin to the luminous arcs observed by Lynds & Petrosian (1986) and Soucail et al. (1987A) and Soucail et al. (1987B) in several galaxy clusters (Paczynśky, 1987). That was spectroscopically confirmed by Soucail et al. (1988). In addition, other wavelengths have been used to observe galaxy cluster lenses (e.g. Smail et al. 2002, Cowie et al. 2002 and Blain et al. 1999 for the sub-millimetre region; Bautz et al. 2000 for the X-Ray range).

At the same time, the development of models describing lensing (Kneib et al. 1996; Bezecourt et al. 1999) made it possible to correct source counts and source fluxes observed through a lens to yield the values that would be found in the absence of the lens. This opened the path to using cluster lenses as natural telescopes to probe the deep Universe to flux limits which would not otherwise be reached with the same time and facilities.

The source plane, observed through the lens, exhibits an apparent surface area dilation that makes it easier to resolve individual sources at a given flux level. This apparent expansion is stronger towards the cluster core and increases with the source plane redshift. In the case of A2218, for example, the magnification in the inner area is greater than a factor of 5, and around a factor of 1.5 or 2 over an area of the order of 70 square arcminutes. In addition, this amplification implies an achromatic increase of the measured flux (due to Liouville's theorem) that improves the limiting flux to which a target field can be observed. This benefit is best appreciated when the lensed area is folded with the number density of sources as a function of flux, as represented in figure 1 (taken from Metcalfe et al. 2003). Parts *a* to *d* show, for example, the area of the sky accessible to the observations of the large ISO "ARCS" lensing survey (Metcalfe et al. 2003; Altieri et al. 1999), as a function of flux, in the absence of a lens (dashed lines), and once the presence of an intervening lens has been taken into account (solid curves). The observations covering A370, A2218 and A2390 are separately treated, along with the merging of the three into a single survey. Parts *e* and *f* indicate the relative number of sources accessible per unit area of sky to a given limiting flux-density, after folding the number density of objects with the flux-dependent survey area for the cases of A2218 and the combined set of three clusters, respectively.

A number of proposals were made with the Infrared Space Observatory (ISO) (Kessler et al. 1996), which could benefit from the lensing effect, and involving a range of galaxy clusters. At the same time, the resulting observations contain a lot of data about the foreground and cluster galaxies. These data are now being exploited for their relevance to the study of the cluster properties.

2. ISO LENSING PROGRAMMES

A total of 420 kiloseconds of ISO observing time were assigned to nine proposals that sought to observe a range of gravitationally lensing galaxy clusters. Five of these programmes directly aimed to take advantage of this phenomenon to probe the background galaxy population. The other four focused on the properties of the clusters themselves: either properties of the cluster galaxies or of the intracluster medium. In table 1 a summary of these ISO programmes is presented, listing their Principal
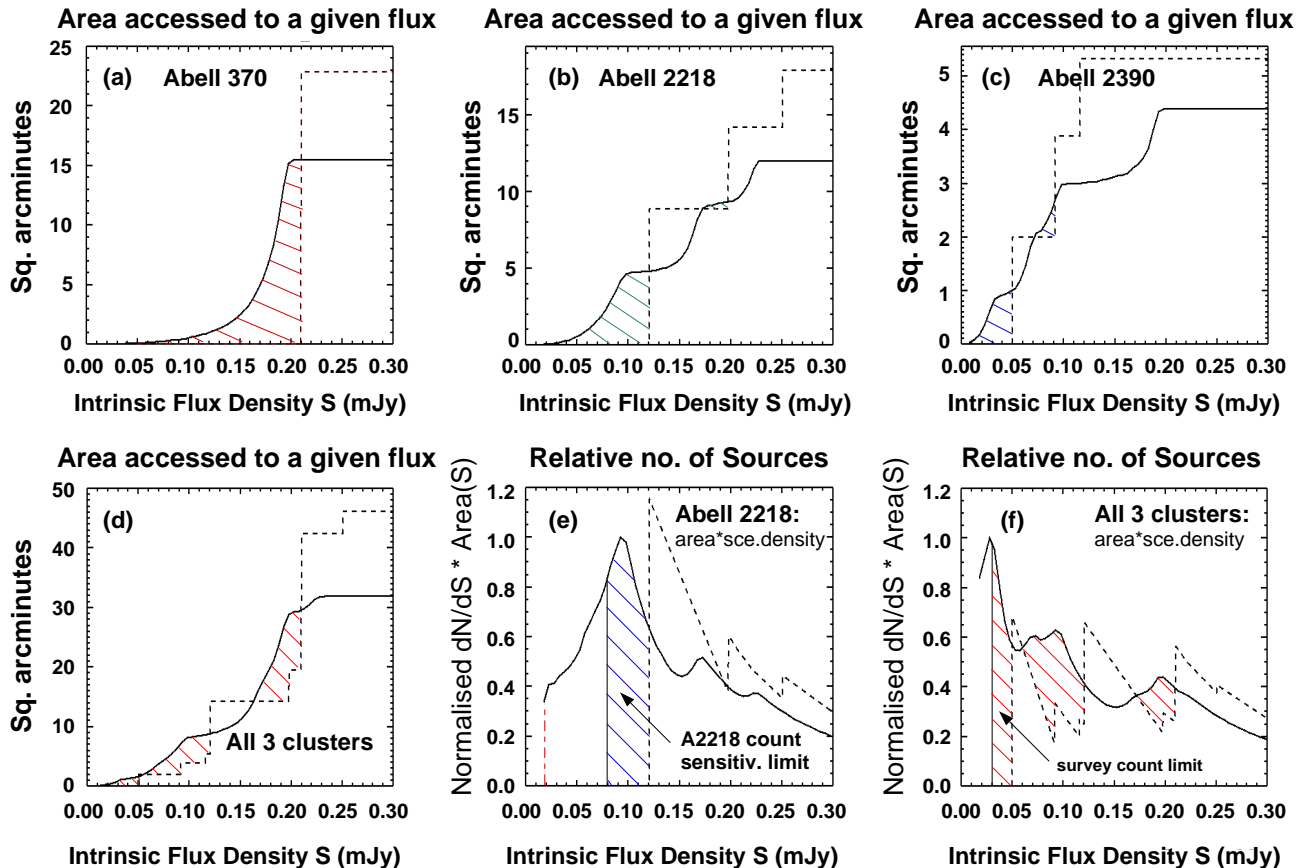
Figure 1. Increased sensitivity due to lensing: in (a), (b) and (c) the dashed line defines, per cluster field, the area of sky accessible to the survey as a function of flux, in the absence of lensing. The profile is stepped because the rastering measurement performed on the sky covered different regions to different depth. The solid curve in each case shows how the area of sky covered depends on the limiting flux after lensing is taken into account. (d) shows the same parameters for the composite survey which results from combining observations on the three clusters. In (e) and (f), the measured distribution of faint MIR sources with flux (Elbaz et al. 2002) has been folded with the previously illustrated flux-dependent accessible areas. The resulting curves: (e) for A2218 and (f) for the three-cluster survey, show the relative number of sources accessible to the survey through lensing. It is seen that a significant population of sources below the unlensed sensitivity limit (dashed line), becomes accessible to the measurement. The peaks in the source-density plots are due to the discontinuities in the sensitivity levels in the "accessible-areas" plots, arising from the raster measuring strategy used (from Metcalfe et al. 2003).

Investigators, their titles, the clusters observed and the time assigned.

A significant part of the information obtained in these programmes is still to be exploited, not only for the original purposes of the programmes, but for other applications as well. Though the first four proposals in the list were intended to observe background objects, they, of course, made deep observations of the clusters themselves.

The ISO ARCS lensing survey made a significant contribution to the number of MIR luminous sources detected with ISO-CAM, detecting about 15% of all deep MIR sources reported. Ongoing exploitation of the data obtained on the clusters (e.g. Coia et al. 2003, Biviano et al. 2003) will yield valuable ISO results for the study of galaxy clusters.

3. SOURCE COUNTS AND IBL RESOLVED

Of the 148 sources detected in the fields of the three clusters used for the ARCS survey, redshifts were available for 89 of them: 6 foreground objects, 40 cluster sources, 31 background objects and 12 stars. For the rest of the sample, a sorting rule was established based on a strong correlation between MIR colour and the cluster-member or non-cluster-member status of the galaxy. It was found that a detection at $15\mu m$ clearly favours a background status. 75% of known-redshift sources seen at 15 μm are background objects. On the other hand, 93% of objects detected only at $7\mu m$ proved to be cluster members.

We concatenate the source counts obtained from the sample of lensed background sources (and the few foreground sources) to the extensive results of other ISOCAM field

Table 1. A list of the ISO programmes relevant to studies of, or through, lensing clusters.

P.I.	Title	Cluster Observed	Assigned Time
Metcalfe	ISO observations of gravitationally lensed arcs	A370, A2218, MS2137, CL2244	56981
Altieri	Ultimate ISOCAM raster on A2390	A2390	143082
Mellier	Arclets in 3 intermediate z clusters	CL0024	25753
Barvainis	High z primeval galaxies lensed by clusters	A2218, A2219	8148
Ivison	A new window on galaxy formation and evolution	A370,A2219, CL2244, MS0440	10348
Biviano	The IR properties of brightest cluster members	A2806,A2870, A2877	78005
Maholtra	Studying gas in gravitational lenses at highz	PKS1830-211, Q2237+030	3362
Cesarsky	Deep imaging of a sample of X-ray galaxy clusters in Hydra	Hydra, A2390	84139
Franceschini	Deep Imaging of Intermediate and High Redshift Clusters	A1689	10044

surveys reported by Elbaz et al. (2002). Integrating in the achieved flux density range from $30\,\mu$Jy to 50 mJy, we resolve $(2.75\pm0.62)\times10^{-9}\,\mathrm{W\,m^{-2}\,sr^{-1}}$, or 55%, of the $15\,\mu$m infrared background, into discrete sources. At $7\,\mu$m we rely entirely on the lensing counts in the limited flux-density range from $14\,\mu$Jy and $460\,\mu$Jy to resolve $(0.49\pm0.2)\times10^{-9}\,\mathrm{W\,m^{-2}\,sr^{-1}}$, or $\sim$10%, of the $6.75\,\mu$m infrared background.

The current measurements and estimated limits to the background radiation from sub-mm to UV wavelengths are presented in figure 2 (adapted from Elbaz et al. 2002). The red and blue points take into account the results of the work reported here, in the context of all the ISOCAM surveys. Our results are completely consistent with the fit derived by Elbaz et al. (2002), extending to fainter flux-densities the experimental confirmation of their model.

The $15\,\mu$m source counts reach very significant levels, showing a steadily increasing excess by a factor of 10 over no-evolution models.

4. FURTHER EXPLOITATION OF ISO DATA

We consider briefly some initial results from the use of ISO lensing data sets to study galaxy clusters, and the possible influence of the cluster environment on galaxy evolution.

The ISO maps of CL0024, obtained by Mellier, have been studied by Coia et al. 2003, in preparation) who have recovered about 50 sources in the $15\,\mu$m map, with 18 cluster galaxies and 2 background sources having redshifts available, and the remaining 30 sources lacking redshift values. Nevertheless, it is already clear that the relationship between cluster-membership and MID IR colour found consistently across the three clusters A370, A2218 and A2390 is not applicable to CL0024. The cluster/non-cluster distribution of 15μm sources is strongly different. Very interestingly, this is very similar behaviour to that reported by Fadda et al. (2000) and Duc et al.(2002) in the case of the cluster A1689, where the cluster is rich in $15\,\mu$m sources. Most of the galaxies detected at 7μm concentrate in the center of the cluster and have similar colours to the overall cluster population. In CL0024, as well as in A1689, there is evidence for a significant MIR analogue of the Butcher-Oemler effect seen in the optical. Though this is a well known phenomenon, it has not been widely investigated in the MIR and this spectral range might bring a better understanding of its nature.

Another important and substantially open field is the comprehensive characterization of the observed MIR sources, either background or cluster galaxies. The results to date indicate that the detected MIR-bright background objects are either AGN powered, or are star forming galaxies, in both cases heavily obscured by dust. The combination of the ISO data with multi-wavelength data available for the well studied lensing cluster fields will facilitate the further classification and characterisation of the background population. Several ISO MIR sources in the fields of A370, A2218, A2390 and CL0024 have been found to have X-Ray counterparts in XMM and/or Chandra maps of the fields, indicating that they are powered by AGNs. These coincidences are under study. A number of ISO sources have submm counterparts, four corresponding to background objects in A370 and A2390 (two sources in each) and one being the central cD galaxy in the core of A2390. They are likely to be luminous dust-obscured star-bursts.

5. CONCLUSIONS

The use of gravitational lensing as a natural telescope is a powerful tool to probe the deep Universe. Eight different ISO programmes obtained data relevant to this theme. The analysis of part of these data has resulted in the resolution into discrete sources of $(2.75\pm0.62)\times10^{-9}\,\mathrm{W\,m^{-2}\,sr^{-1}}$ of the $15\,\mu$m infrared background light, and $(0.49\pm0.2)\times10^{-9}\,\mathrm{W\,m^{-2}\,sr^{-1}}$ of the $7\,\mu$m infrared background light.

But this is not all. The great value of the data for studies of the galaxy clusters themselves begins to be realised, with potential to yield unprecedented results for clusters with redshifts up to 0.4, and the possibility to further characterise a MIR Butcher-Oemler effect suggested by Fadda et al. (2000) from the ISO data on the z= 0.18 cluster Abell 1689. Early results on the z=0.39 cluster CL0024 are very encouraging.

The combination of ISO MIR data on these novel, very well studied, cluster fields, with available multi-wavelength data can contribute significantly to characterisation of galaxy populations and galaxy evolution.
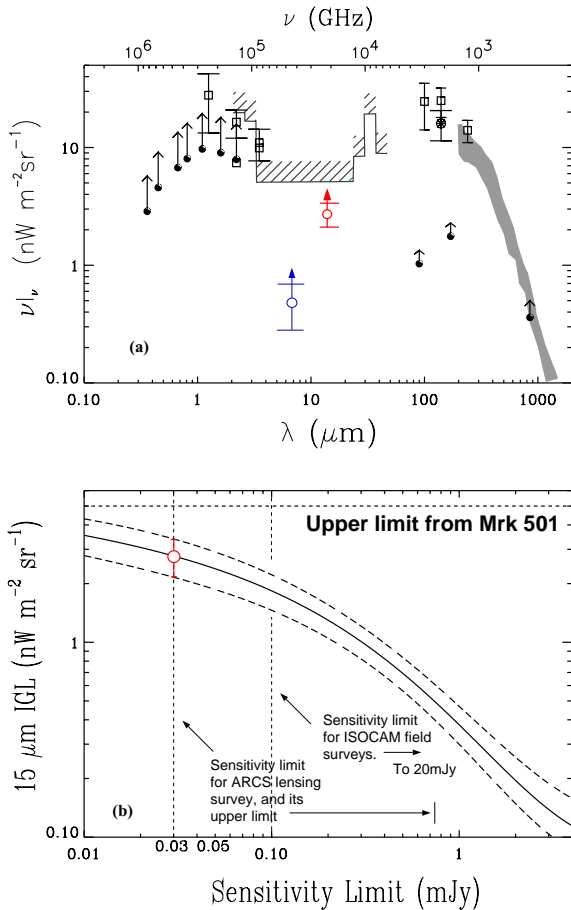
Lynds, R., Petrosian, V. 1986, Bull. Am. Astr. Soc. 18, 1014

Metcalfe, L., Kneib, J,-P., McBreen, B. et al. 2003, in preparation

Paczyński, B. 1987, Nature, 325, 572

Smail, I., Ellis, R., Blain, A. W., Kneib, J.-P. 2002, MNRAS, 331, 495

Soucail, G., Fort, B., Mellier, Y., & Picat, J. P. 1987, A&A, 172, L14

Soucail, G., Mellier, Y., Fort, B., Mathez, G., & Hammer, F. 1987, A&A, 184, L7

Soucail, G., Mellier, Y., Fort, B., Cailloux, M. 1988, A&AS, 73, 471

Young, P., Gunn, J.E., Oke, J.B., Westphal, J., Kristian, J. 1980, ApJ 241, 507

Figure 2. *Figure is adapted from Elbaz et al. (2002), showing results from Metcalfe et al. (2003). (a) presents limits to, and measurements of, the background radiation from UV to sub-millimetre wavelengths, as described in Elbaz et al. (2002). The values of the integrated background light at 7 and 15 μm, calculated from lensing source counts, have been plotted on this graph. (b) shows the 15 μm resolved IBL value plotted over the Elbaz et al. (2002) fit to the counts of other ISO-CAM deep surveys. The lensing data point extends the flux-limit of the observations and remains consistent with the fit. The dashed lines correspond to 1-σ error bars obtained by Elbaz et al. (2002) fitting the upper and lower limits of the source counts from other surveys. The error bars on the overplotted lensing data point were obtained by integrating over the upper and lower limits of the differential source counts.*

REFERENCES

Altieri, B., Metcalfe, L., Kneib, J-P. et al. 1999, A&A, 343, 65

Bautz, M.W., Malm, M.R., Baganoff, F.K. et al. 2000, ApJ, 543, L119

Bézecourt, J., Kneib, J. P., Soucail, G., & Ebbels, T. M. D. 1999, ApJ, 347, 21

Biviano et al. 2003, in preparation

Blain, A.W., Kneib, J.-P., Ivison, R.J. & Smail, I. 1999, ApJ 512, L87

Coia et al. 2003, in preparation

Cowie, L., Barger, A., Kneib, J.-P., 2002, ApJ, 123, 2197

Duc, P.-A., Poggianti, B. M., Fadda, D. et al. 2002, A&A, 382, 60

Elbaz, D., Cesarsky, C.J., Chanial, P. et al. 2002, A&A, 384, 848

Fadda, D., Elbaz, D., Duc, P.-A. et al. 2000, A&A, 361, 827

Kessler, M.F., Steinz, J.A., Anderegg, M. et al. 1996, A&A, 315, L27

Kneib, J-P., Ellis, R.S., Smail, I., Couch, W.J., Sharples, R.M. 1996, ApJ, 471, 643

A FAR-INFRARED VIEW OF THE LOCKMAN HOLE FROM ISOPHOT

Giulia Rodighiero[1], Dario Fadda[2,3], Alessandra Gregnanin[1], Carlo Lari[4], and Alberto Franceschini[1]

[1]Dipartimento di Astronomia, Università di Padova, Vicolo dell'Osservatorio 2, I-35122 Padova, Italy
[2]Caltech, SIRTF Science Center, MC 220-6, Pasadena, CA 91126, USA
[3]Instituto de Astrofísica de Canarias (IAC), Via Lactea S/N, E-38200 La Laguna, Spain
[4]Istituto di Radioastronomia del CNR, via Gobetti 101, I-40129 Bologna, Italy

ABSTRACT

An important advance in the knowledge of the nature of galaxies is possible only using mid- and far-infrared data. In particular, the deep and extended surveys performed by the satellite ISO are suited for this kind of study. We present our preliminary results of the analysis of the PHOT $90\,\mu$m data in the Lockman Hole with a recently developed technique (Lari et al. 2001). The survey covers an area of $40' \times 40'$, and is complementary to the shallow survey in the mid-infrared by ISOCAM. We are able to detect 36 sources down to a flux of $\sim$20 mJy. In particular, we discuss the cross-correlations between the far- and the mid- infrared sources. For the sample of sources detected in both IR bands, it becomes possible to study in detail the SEDs exploiting optical data (photometry in several bands and spectroscopy).

1. INTRODUCTION

The infrared and submillimeter window from 1 to 1000 μm is a powerful instrument to study the early phases of galaxy evolution.

With the advent of the Infrared Space Observatory (ISO, Kessler et al. 1996) the improved resolution and sensitivities of the detectors made deep infrared surveys possible that for the first time allowed to study the evolution of faint IR galaxies at cosmological distances, both in the mid and in the far infrared. 15 μm ISOCAM-LW3 counts at different flux levels reveal a consistent deviation from the Euclidean slope (Elbaz et al. 1999), which has been interpreted as the presence of a strongly evolving mid-IR population of starburst galaxies (Franceschini et al. 2001, Gruppioni et al. 2002) . Similar findings seem to emerge from different ISOPHOT surveys in the 90 and 175 μm channels (Efsthatiou et al. 2000, Mathsuhara et al. 2000, Dole et al. 2001). The 90 μm filter in particular is crucial, as the Spectral Energy Distribution (SED) of actively starforming galaxies peaks around 60 and 100 μm. For luminous infrared galaxies, more than 80% of the flux can be emitted in the far-IR, and the peak of the far-IR emission becomes a measure of the bolometric luminosity of such galaxies, and a good estimator of their star formation rate. The long-standing problem with ISOPHOT 90 μm observations was the difficulty to reduce the data taking into account all the instrumental effects (mainly due to cosmic ray impacts on the detector), preventing to get highly reliable samples (spurious detections can affect the final source lists). Here we present our new method for the reduction of ISOPHOT C100 data, which has been developed starting from the code designed for ISOCAM LW data by Lari et al. (2001). We report on our analysis of the ISOPHOT 90 μm Lockman Hole survey, a region particularly suited for the detection of faint infrared sources due to its low cirrus emission. The good quality of the data and a careful reduction allow us to reach faint detection limits ($\sim$ 20 mJy). We focus in particular on the implications for the evolutionary models as derived from galaxy counts. Our results seem to favour a scenario dominated by a strongly evolving population, quite in agreement with the model discussed by Franceschini et al. (2001).

2. THE LOCKMAN HOLE OBSERVATION STRATEGY

The Lockman Hole was originally selected for its high ecliptic latitude ($|\beta| > 50$, to reduce the impact of zodiacal dust emission) and low cirrus emission. This region presents the lowest HI column density in the sky, and turns out to be particularly suited for the detection of faint infrared sources. In the past few years these advantages enhanced the study of the Lockman Hole at other wavelengths, making it a powerful region to study the nature and the statistical properties of faint distant galaxies, via a multi-frequency approach. Today the spectral coverage goes from the X rays (Hasinger et al. 2001), to the optical (Fadda et al. in preparation), the mid-infrared (Fadda et al. 2002), the far-infrared (Kawara et al. 1998), the submillimeter (Scott et al. 2002), until the radio (De Ruiter et al. 1997). The spectroscopic information is still sparse.

Two different regions in the Lockman Hole have been observed by ISOPHOT on board the Infrared Space Observatory (ISO; Kessler et al. 1996). Each of the two fields, called LHEX and LHNW, covers an area of $\sim 44' \times 44'$ and has been surveyed at two far-infrared wavelengths with the C100 and C200 detector (respectively at 90 and 175 μm, with the C_90 and C_160 filters), in the P22 raster configuration. We focused our analysis on the LHEX field, which is a mosaic composed of four rasters each covering an area of $\sim 22' \times 22'$, observed in the PHT22 staring raster map mode. The ISOPHOT detector was moved across the sky describing a grid pattern, with about half detector step in both directions (corresponding to 1.5 detector pixel). This strategy improves the reliability of source detections as each sky position is observed twice in successive pointings.
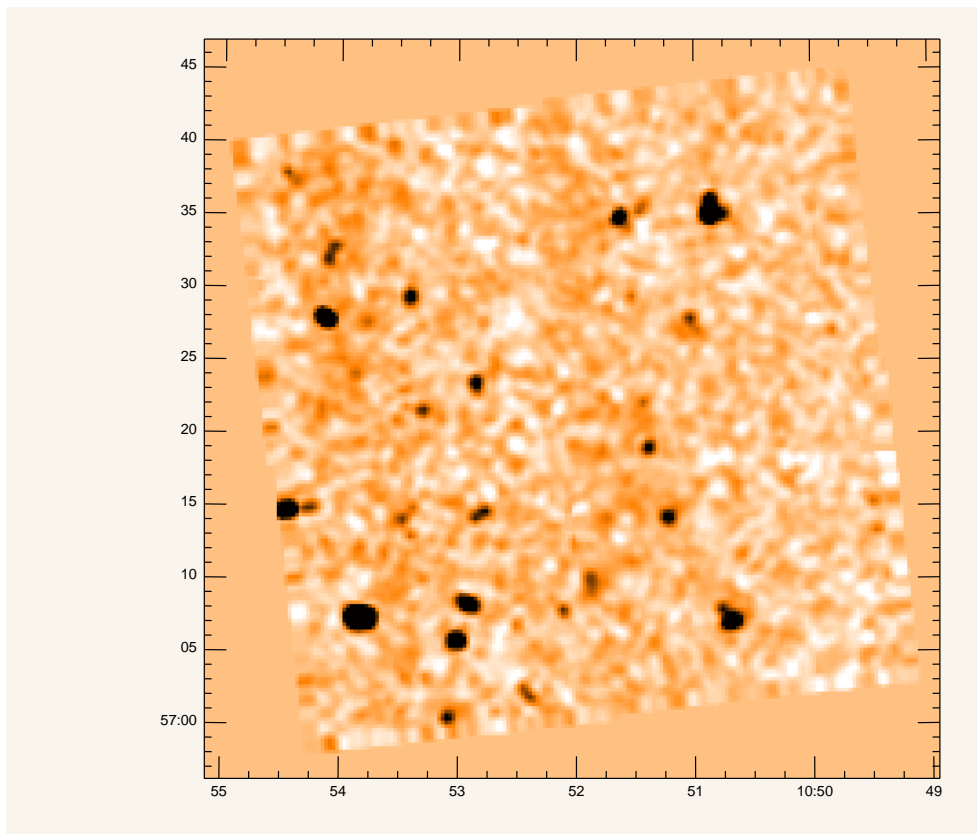
Figure 1. ISOPHOT 90 μm map in the Lockman Hole. North is up, East is to the left.

3. A NEW TOOL FOR THE REDUCTION OF PHOT-C DATA

As known, the reduction of ISO data requires a careful treatment of all the external and instrumental effects affecting the detectors. The results recently obtained by Lari et al. (2001) in developing a reduction technique for ISOCAM LW data, prompted us to apply the same approach to the analysis of ISOPHOT data. We will not enter in the details of the algorithm and of the computation, which are described in Lari et al. (2001). Instead, here we will discuss the main aspects and implications of this new procedure that is especially designed for the detection of faint sources.

As for the ISOCAM LW detector, in the ISOPHOT C detectors two main effects must be considered, produced by cosmic ray impacts (*glitches*) and transient behaviour (i.e. the slow response of the detector to flux variations), respectively. The method discussed by Lari et al. (2001) was mainly developed to describe and overcome these problems. It is based on the assumption that the incoming flux of charged particles generates transient behaviours producing two different time scale effects: a fast (**breve**) and a slow (**lunga**) one. Applying this model we look at the time history of each detector pixel and the code finds the stabilization background level. Then it models the glitches, the background and the sources with all the transients over the whole pixel time history.

The application to PHOT-C data is not a simple translation of what has been done for CAM-LW. If the approach is the same, some peculiarities of the far-infrared detector need to be treated with a more suitable technique. However, we found that the description of transients with the equations used in the case of CAM pixels works also in fitting PHOT-C data (after adapting the temporal and charge parameters).

4. APPLICATION TO THE LOCKMAN HOLE

The Lockman Hole 90 μm field represent a good dataset to test the performance of our reduction technique. The long integration times (∼ 16 sec for each raster position) and the redundancy allow an accurate evaluation and modeling of any transient effects, on both long and short time scales. This is a performant strategy for the detection of faint sources: shorter observing times affect the signal-to-noise ration and make strong glitches hide real sources.

4.1. THE SOURCE CATALOGUE

The final catalogue obtained with our method contains 36 sources detected at 90 μm in the Lockman Hole, over an area of 0.5 □°. All sources have a signal-to-noise ratio greater than 3. In Fig. 1 we show the final mosaic map obtained combining together the four raster sub-maps. The catalogue will be pre-
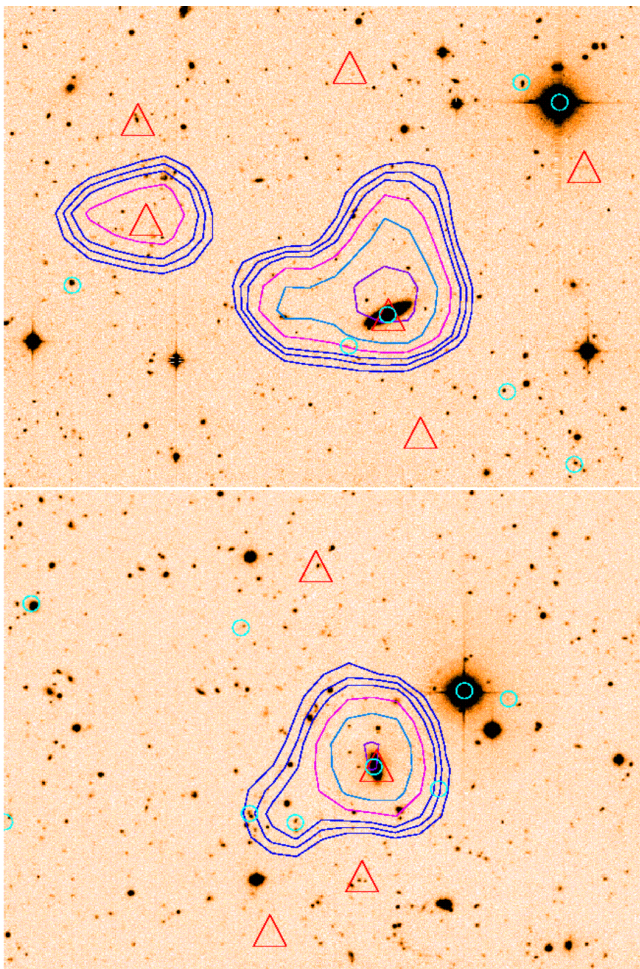
Figure 2. Optical R-band image with superimposed the 90 μm contours. Red triangles are radio detections (De Ruiter et al. 1997), open blue circles are CAM LW3 detection.

sented in Rodighiero et al. (2002, in preparation). All sources have been extracted from the map and confirmed by visual inspection on the pixel history (by two independent people). This approach provides an highly reliable catalogue.

5. IDENTIFICATIONS

Given the low spatial resolution of ISOPHOT detectors, it is difficult to make a direct cross-correlation between far-IR and optical sources. However, these identifications are important in order to obtain informations about the spectroscopic redshifts of our sample. A powerful way to associate a far-IR source to its optical counterpart is to look at the catalogue positions of the same field in another wavelength. In our case, for example, we can use the informations coming from ISO-CAM LW3 15 μm maps (see Fadda et al., this volume and Fadda et al. 2002 in preparation) of the same region surveyed at 90 μm. Moreover, the Lockman Hole have been observed in the radio (De Ruiter et al. 1997), and given the known far-IR/radio correlations, we can use also this high resolution map to find the far-IR counterparts. We show in Fig. 2 two optical R-band images with super-

imposed the 90 μm contours. It is evident that in the large beam of the PHOT detector pixels we can find more optical sources. We report also radio (red triangles) and CAM LW3 (open blue circles) detections. In these examples the associations between the optical and the IR source is evident.
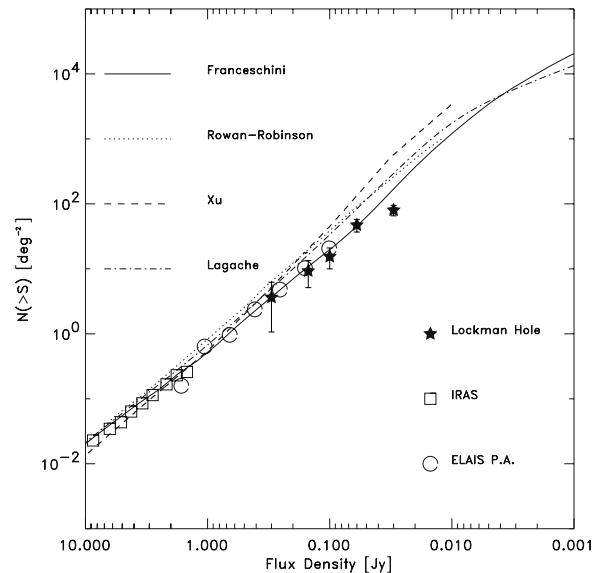

Figure 3. Integral 90 μm counts, compared with different model predictions.

5.1. SOURCE COUNTS

Notwithstanding the small area covered by the present study ($\sim$0.5 $\square^\circ$), we have computed the 90 μm source counts down to a flux level of 30 mJy. The integral counts have been obtained by weighting each single source for its effective area. The reported errors represent the Poissonian term of the uncertainties, and have to be considered as lower limits to the global source counts errors. The computed values of the integral counts at different flux levels are plotted in Fig. 3 as stars. Here we compare our counts with the results from other surveys: the preliminary analysis from the ISOPHOT ELAIS survey (Efsthatiou et al. 2000, open circles), and the counts derived from the IRAS 100 μm survey (open triangles).

Our data are in good agreement with previous results, showing a good overlap in the common flux range.

The present results seem to confirm the existence of an evolving population of IR galaxies. The solid line in Fig. 3 that nicely fits the 90 μm counts, represents the model from Franceschini et al. (2001). For comparison we report other models: the dot-dashed line in Figure 3 comes from Lagache et al. (2002), the dashed line from Xu et al. (2001), the dotted line is the model by Rowan-Robinson et al. (1999).

The Franceschini et al. (2001) model reproduces the IR counts assuming the contribution of three population components characterized by different physics and evolutionary prop-

erties. The main contribution come from non-evolving spirals and from a fast evolving population including type-II AGNs and starburst galaxies. A third component considered are type-I AGNs. The fraction of the evolving starburst population is assumed to be ~10 percent of the total (consistent with the local observed fraction of interacting galaxies). In this scenario, every galaxy is expected to spend most of its life in a quiescent phase. However occasional interactions with other sources put it in a short active starbursting phase (few to several 10^7 years). The interpretation of this cosmological evolution is simply related to a geometrical effect that increases the probability of interactions in the past.

Let us note that our statistics is limited to an area of about $0.5 \square^\circ$, and that we need a wider sample to better constrain the far-IR source counts. We are planning to reduce other ISO-PHOT C100 surveys, like the second Lockman Hole (LHNW) and the ELAIS fields. With our method we foresee to reach fainter flux limits than the preliminary analysis (Efsthatiou et al. 2000). A first reduction of few ELAIS rasters indicates that we are able to detect sources at a level of ~50 mJy.

Another limit of the present analysis is related to the resolution of the ISOPHOT detector and to its low sensitivities. In the near future, deeper far-IR observations will be possible with SIRTF, while a proper characterization of the faint far-IR population will require the Herschel's better spatial resolution.

REFERENCES

De Ruiter H. R., Zamorani G., Parma P., Hasinger G., Hartner G., Truemper J., Burg R., Giacconi R., Schmidt M., 1997 A&A, 319, p.7-17

Dole H., Gispert R., Lagache G., Puget J.-L., Bouchet F. R., Cesarsky C., Ciliegi P., Clements D. L., Dennefeld M., Desert F.-X., Elbaz D., Franceschini A. et al., 2001 A&A, 372, p.364-376

Efstathiou A., Oliver S., Rowan-Robinson M., Surace C., Sumner T., Heraudeau P., Linden-Vornle M. J. D., Rigopoulou D., Serjeant S. et al., 2000 MNRAS, 319, Issue 4, pp. 1169-1177

Elbaz D., Cesarsky C. J., Fadda D., Aussel H., Desert F. X., Franceschini A., Flores H., Harwit, M., Puget J. L., Starck J. L., Clements D. L., Danese L., Koo D. C., Mandolesi R., 1999, A&A 351, L37-L40

Fadda D., Flores H., Hasinger G., Franceschini A., Altieri B., Cesarsky C. J., Elbaz D., Ferrando Ph., 2002 A&A, 383, p.838-853

Franceschini A., Aussel H., Cesarsky C. J., Elbaz D., Fadda D., 2001 A&A, 378, p.1-29

Gruppioni C., Lari C., Pozzi F., Zamorani G., Franceschini A., Oliver S., Rowan-Robinson M., Serjeant S., 2002 MNRAS 335, Issue 3, pp. 831-842

Hasinger G., Altieri B., Arnaud M., Barcons X., Bergeron J., Brunner H., Dadina M., Dennerl K., Ferrando P., Finoguenov A., Griffiths R. E., Hashimoto Y. et al., 2001 A&A, 365, p.L45-L50

Kawara K., Sato Y., Matsuhara H., Taniguchi Y., Okuda H., Sofue Y., Matsumoto T., Wakamatsu K., Karoji H., Okamura S., Chambers K. C., Cowie L. L., Joseph R. D., Sanders D. B., 1998 A&A, 336, p.L9-L12

Kessler M. F., Steinz J. A., Anderegg M. E., Clavel J., Drechsel G., Estaria P., Faelker J., Riedinger J. R., Robson A., Taylor B. G., Ximenez de Ferran S.,1996 A&A, 315, L27-L31

Lagache G., Dole H., Puget J. L., astro-ph/0209115

Lari C., Pozzi F., Gruppioni C., Aussel H., Ciliegi P., Danese L., Franceschini A., Oliver S., Rowan-Robinson M., Serjeant, S., 2001, MNRAS 325, 1173L

Matsuhara H., Kawara K., Sato Y., Taniguchi Y., Okuda H., Matsumoto T., Sofue Y., Wakamatsu K., Cowie L. L., Joseph R. D., Sanders D. B., 2000 A&A, 361, p.407-414

Rowan-Robinson M., 1999, in "ISO Survey of a Dusty Universe", Proceedings of a Ringberg Workshop Held at Ringberg Castle, Tegernsee, Germany, , Edited by D. Lemke, M. Stickel, and K. Wilke, Lecture Notes in Physics, vol. 548, p.129

Scott S. E., Fox M. J., Dunlop J. S., Serjeant S., Peacock J. A., Ivison R. J., Oliver S., Mann R. G., Lawrence A., Efstathiou A., Rowan-Robinson M., Hughes D. H., Archibald E. N., Blain A., Longair M., 2002 MNRAS, 331, Issue 4, pp. 817-838

Xu C., Lonsdale C. J., Shupe D. L., O'Linger J., Masci F., 2001 ApJ, 562, Issue 1, pp. 179-207

THE EUROPEAN LARGE AREA ISO SURVEY: 90 MICRON NUMBER COUNTS

Philippe Héraudeau[1], Carlos del Burgo[1], Manfred Stickel[1], Andreas Efstathiou[2], Michael Rowan-Robinson[2],
Csaba Kiss[3], Péter Ábrahám[3], Sebastian Oliver[4], Ulrich Klaas[1], and Dietrich Lemke[1]

[1] Max-Planck-Institut Für Astronomie, Königstuhl 17, Heidelberg, Germany
[2] Astrophysics Group, Blackett Laboratory, Imperial College, Prince Consort Rd, London SW7 2BW, UK
[3] Konkoly observatory of the Hungarian Acadamy of Sciences, P.O.Box 67, H-1525 Budapest, Hungary
[4] Astronomy Centre, CPES, University of Sussex, Falmer, Brighton BN1 9QJ , UK

ABSTRACT

The European Large Area ISO Survey (ELAIS) was the largest single Open Time project conducted by ISO, mapping an area of 12 square degrees at $15 \mu m$ with ISOCAM and at 90μ with ISOPHOT. We first present the data analysis of the $90 \ \mu m$ survey. We show comparisons with model prediction for standard stars and with COBE/DIRBE for surface brightnesses of individual ELAIS fields and with the IRAS FSC catalog for 35 sources in common. The large number of rasters necessary to cover the wide ELAIS areas allows to compute a relative uncertainty for the calibration based on the FCS of typically 7%. From the comparison with standard stars model predictions, the absolute calibration is shown to be better than 15%.

The survey is 1.5 order of magnitude deeper than the IRAS $100 \mu m$ survey and is expected to provide constraints on the formation and evolution of galaxies.

Finally, we present $90 \ \mu$m number counts from a reliable subset of the detected sources. ELAIS number counts are compared to the evolutionary models of Guiderdoni (1998) and Rowan-Robinson (2001).

Key words: ISOPHOT; survey; galaxy evolution; Methods: data-analysis

1. OBSERVATIONS

The ELAIS survey was carried out in four main areas (three in the northern and one in the southern hemisphere) and some smaller areas of special scientific interest. The data consists of a number of P22 staring raster maps performed with the 3×3 array of the ISOPHOT instrument on-board ISO. The pixel size of the C100 detector is $43.5'' \times 43.5''$ on the sky and the C_90 filter with reference wavelength $90 \mu m$ was used (see Oliver et al. 2000) for a complete description of the survey at 15,90 and $175 \mu m$).

The area covered by each raster is typically 20×40 square arcminutes and the 4 largest fields are about 2.5 square degrees, N3 having the lowest coverage is only 2.1 square degree.

2. DATA PROCESSING

The data were first processed with PIA (PHT Interactive Analysis) version 9.1 using the OLP10 calibration files with however the improved dark signal and reset interval correction, and the consideration of by-passing sky light on the FCS (see Héraudeau et al. (2002a), del Burgo et al. (2002a) and del Burgo et al. (2002b) for details on ISOPHOT calibration).

The data reduction from ERD (Edited Raw Data) to SCP (Signal per Chopper Plateau) was performed using the so-called pairwise method developed by Manfred Stickel. The distribution of the difference between consecutive read-outs is used instead of making linear fits to the whole ramps. After rejecting the first 10% of the data stream which can be affected by transient, the mode of the distribution is estimated with myriad technique (Kalluri & Arce 1988) as the final signal for each raster position. This method has the advantage to be more robust against glitches caused by cosmic rays and which might create spurious sources in the data stream.

For each field, the relative uncertainty coming from the FCS calibration was computed as the mean absolute deviation of the average sky background of all rasters and is typically 7%.

3. SOURCE DETECTION AND CLASSIFICATION

The source detection was performed using the Sextractor software, version 2.2.2 (Bertin & Arnouts 1996), on the final map. To ensure the reliability of the sources detected by Sextractor, we confront them to eye-balled classification based on the time sequence analysis of the data streams (See Surace et al. 1999). For each source detected by Sextractor we look for the classifications of detections around the central position within the size of the C100 detector array. We retain sources which were classified at least twice as a source and with a signal-to-noise ratio larger then 3.

4. CALIBRATION

4.1. STANDARD STARS

In order to better determine the ELAIS calibration (as well as the general ISOPHOT calibration) three stars (HR6132, HR6464 and HR5981) close to the ELAIS fields were observed in mini-raster mode (a 3×3 raster with the star positioned at the centre of a different pixel in each pointing). The faintest of the stars (HR598) was observed twice on the same ISO orbit. To increase the sample of measurements and thus the reliability of the comparison we selected all other standard stars from the archive also observed in mini-raster mode at $90 \mu m$. These stars also formed part of the ISO ground based preparatory programme. Models for their far-IR spectra were constructed by

fitting near-IR data and extrapolating to longer wavelengths as ν^2 (Hammersley et al. 1998). A more empirical approach was given by Cohen et al. (1999). The predicted stellar fluxes lie in the range 0.06 - 10Jy. Tab. 1 shows the list of stars and the characteristics of the measurements as well as predicted fluxes. The integration time per pointing in these mini-rasters (from 40 to 72s) is longer than that used for the bulk of the ELAIS survey in order to obtain an accurate determination of fluxes to establish the ISOPHOT calibration. The observations of calibration stars were processed in the same way as the survey rasters. Results of the comparison are given in Tab. 1 as the ratio between measured (based on the FCS) and theoretical fluxes. When two model predictions were available, we used their mean to compute the ratio. The two measurements on *HR5981* are in agreement within 5%. ISOPHOT fluxes are systematically higher than the predicted ones and the mean ratio is 1.12 ± 0.11.

4.2. COMPARISON TO COBE/DIRBE

The extensions of the large ELAIS fields make them appropriate for a comparison of their sky background brightnesses with COBE/DIRBE without being hampered by the lower resolution of the latter. For a systematic comparison of ISOPHOT versus DIRBE surface brightnesses see Héraudeau et al. (2002a).

Fig. 1 shows the comparison of DIRBE versus ISOPHOT surface brightnesses. Error bars for DIRBE are typically equal to $0.06 MJy/sr$. Error bars for Phot come from the rms of the rasters sky background level for each series of measurement and are typically $0.2 MJy/sr$.

The relationship is well fitted with a straight light of the form:

$$\text{SB(ISOPHOT)} = 0.55 \pm 0.56 + 1.30 \pm 0.16 \times \text{SB(DIRBE)}$$
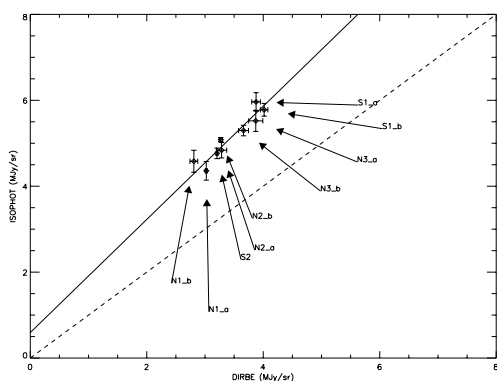

Figure 1. Comparison of ISO and COBE/DIRBE surface brightnesses for the ELAIS fields. The largest fields (N1,N2,N3 and S1 are divided into two sets of measurements ($N1_a$, $N1_b$, etc...) which were performed at different period of the year and therefore may have different Zodiacal light contribution. DIRBE values were interpolated at $90\mu m$. The solid line is the result of fitting the points with a straight line. The dotted line represents a slope of unity.

4.3. COMPARISON WITH *IRAS* SOURCES

While the ELAIS fields were chosen to avoid strong infrared sources, there are a number of IRAS $100\mu m$ sources in the PSC and FSC which were detected in the survey. The fluxes of these 35 sources lie in the range $0.2 Jy \leq S(100) \leq 2.1 Jy$. Fig. 2 shows the comparison with the FSC catalogue which is the more accurate at this faint level. All common sources have low (the flux is an upper limit) or intermediate IRAS quality flags. Color correction factors were computing from the IRAS 4-band Spectral Energy Distribution and IRAS and ISOPHOT filter profiles.

Optical identifications of these sources appear to be galaxy pairs or galaxies. Three of them are stars. The mean difference between IRAS and ISOPHOT is 0.086 Jy and the standard deviation is 0.20 Jy for IRAS data with intermediate quality flag (2) only.
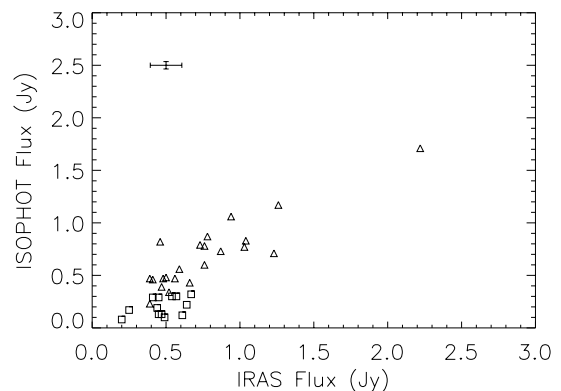

Figure 2. Comparison of ISOPHOT and IRAS/FSC fluxes at 90 micron for 35 common sources in the ELAIS fields. The $90\mu m$ fluxes of the IRAS sources are estimated by linearly interpolating between the color-corrected 60 and $100\mu m$ fluxes. Squares and triangles correspond to IRAS sources with quality flag equal to 1 (upper limit) and 2 (intermediate quality). Typical error bars are indicated in the upper-left part of the diagram.

4.4. CONCLUSION ON CALIBRATION

We rescaled our photometry according to the difference found for standard stars (i.e. a factor 1.12). This correction also goes towards the same direction than the slope of the relationship found for surface brightnesses between ISO and DIRBE which is somewhat larger (a factor 1.30). As we are mainly interested in calibrating point sources we do not use the scaling factor coming from the surface brightnesses comparison which may involve additional uncertainties coming from the determination of solid angles.

5. NUMBER COUNTS

The resulting integral counts are given in Fig. 3 (points) where are also plotted the IRAS counts (see Efstathiou et al. 2001).

Table 1. *The list of standard stars used to check the FCS calibration with theoretical values. TDT numbers of measurements, name of stars, exposure time, size of the mini-rasters, model predictions from M. Cohen ('MC') and P. Hammersley ('PH') as well as ISOPHOT fluxes and their uncertainties are indicated. "Ratio" is the ratio between measured and predicted fluxes. When two model predictions were available, we used their mean to compute the ratio. "Iras" is the IRAS flux extrapolated from the $60\mu m$ flux when the quality flag was good.*

Measurement	Name	Exposure	RI	Size	$F(MC)$	$F(PH)$	Pht	$e_p ht$	Ratio	Iras
		sec	sec		Jy	Jy	Jy	Jy	–	Jy
08602417	HR5340	37.00	0.12	5	9.308	9.029	9.589	0.360	1.046	8.573
10503417	HR6705	72.00	0.50	5	2.013	1.904	2.424	0.139	1.237	2.001
27502117	HR5340	72.00	0.25	5	9.308	9.029	9.593	0.233	1.046	8.573
29301005	HR7310	72.00	4.00	5	0.258	0.268	0.330	0.022	1.281	0.251
39103002	HR8775	72.00	0.25	5	4.961	5.096	5.777	0.143	1.149	5.300
65701318	HR1654	72.00	1.00	3	0.713	–	0.744	0.026	1.044	0.666
72701418	HR7980	72.00	1.00	3	0.517	–	0.477	0.024	0.923	0.488
77200361	HR5981	40.00	2.00	3	–	0.063	0.071	0.015	1.131	–
77200364	HR5981	40.00	2.00	3	–	0.063	0.066	0.010	1.058	–
78300465	HR6464	40.00	2.00	3	–	0.120	0.157	0.020	1.310	–
78300677	HR6132	40.00	2.00	3	–	0.288	0.323	0.023	1.121	–
63801807	HR7451	54.00	1.00	3	–	0.0075	0.0427	0.010	5.696	–

ELAIS counts are corrected for incompleteness estimated from the number of recovered simulated sources on the maps.

5.1. COMPARISON WITH EVOLUTIONARY MODELS

In figure 3 we also compare the observed counts with the evolutionary models of Rowan-Robinson (1999) and Guiderdoni et al. (1998).

The model of Rowan-Robinson includes four spectral components: infrared cirrus (emission from interstellar dust), an M82-like starburst, an Arp220-like starburst and an AGN dust torus.

The model of Guiderdoni et al. is set within the framework of hierarchical growth of structures according to the cold dark matter model, and extends earlier studies to the IR/submm wavelength regime. In Fig. 3 we plot the prediction from their models A and E. The latter model incorporates a heavily extinguished (ULIRG) population, assumed to dominate at high redshift in order to account for the far-ir background.

6. SUMMARY AND CONCLUSION

We have re-analysed ELAIS $90\mu m$ data with the so-called "pairwise" method which is more robust against glitches than the usual ramp fitting. We selected sources with a signal-to-noise ratio larger than 3 and which were classified as a real source by at least 2 people to ensure their reliability.

The ELAIS counts extend the IRAS counts by 1.5 order of magnitude in flux. The slope of the counts is consistent with the strong evolution seen in other infrared and submillimeter surveys.

Within the uncertainties associated with the flux calibration of the survey, the counts agree with the strongly evolving models of Rowan-Robinson (1999) and Guiderdoni et al. (1998) favouring the model E of the latter.
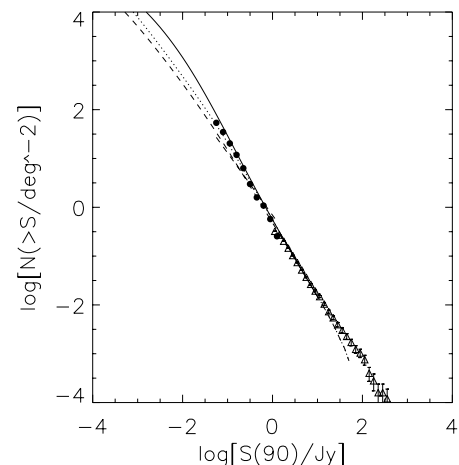

Figure 3. ELAIS $90\mu m$ number counts. The solid line represents the model of Rowan-Robinson (1999), the dashed and dotted lines show model A et E respectively of Guiderdoni et al. (1998). Iras number counts are also plotted (triangles).

REFERENCES

Del Burgo, C., Ábrahám, P., Klass, U. and Héraudeau., P., 2002a, ESA SP-428 , in press.

Del Burgo, C., 2002b, this volume.

Efstathiou, A. et al., MNRAS, 2000, Vol 319,4, p. 1169-1177.

Guiderdoni, B., Hivon, E., Bouchet, F.R., Maffei, B., MNRAS, 1998, 295, 877.

Héraudeau, Ph., Ábrahám, P., Klaas, U., Kiss, C., 2002a, ESA, SP-428, in press

Héraudeau, Ph. Ábrahám, P., Klaas, U., Del Burgo , C. , 2002b, ESA SP-428, in press.

Kalluri, S. and Arce, G.R., 1998, IEEE Transactions on Signal Processing 46 ,322.

Rowan-Robinson, M. , 2001, Lecture Notes in Physics, vol. 548, p.129.

Oliver, S. and ELAIS consortium, MNRAS, 2000, Vol. 316,4, p. 749-767.

Surace, C., Héraudeau, Ph., U., Lemke, D., Oliver, S., Rowan-Robinson ELAIS, ISOPHOT results, 1999, ESA SP-427,Vol. 2, p. 1059-1062.